How Cells Count using Social Media:

Study of Density-dependent Effects on Growth and Differentiation of Embryonic Stem Cells

Pim van den Bersselaar

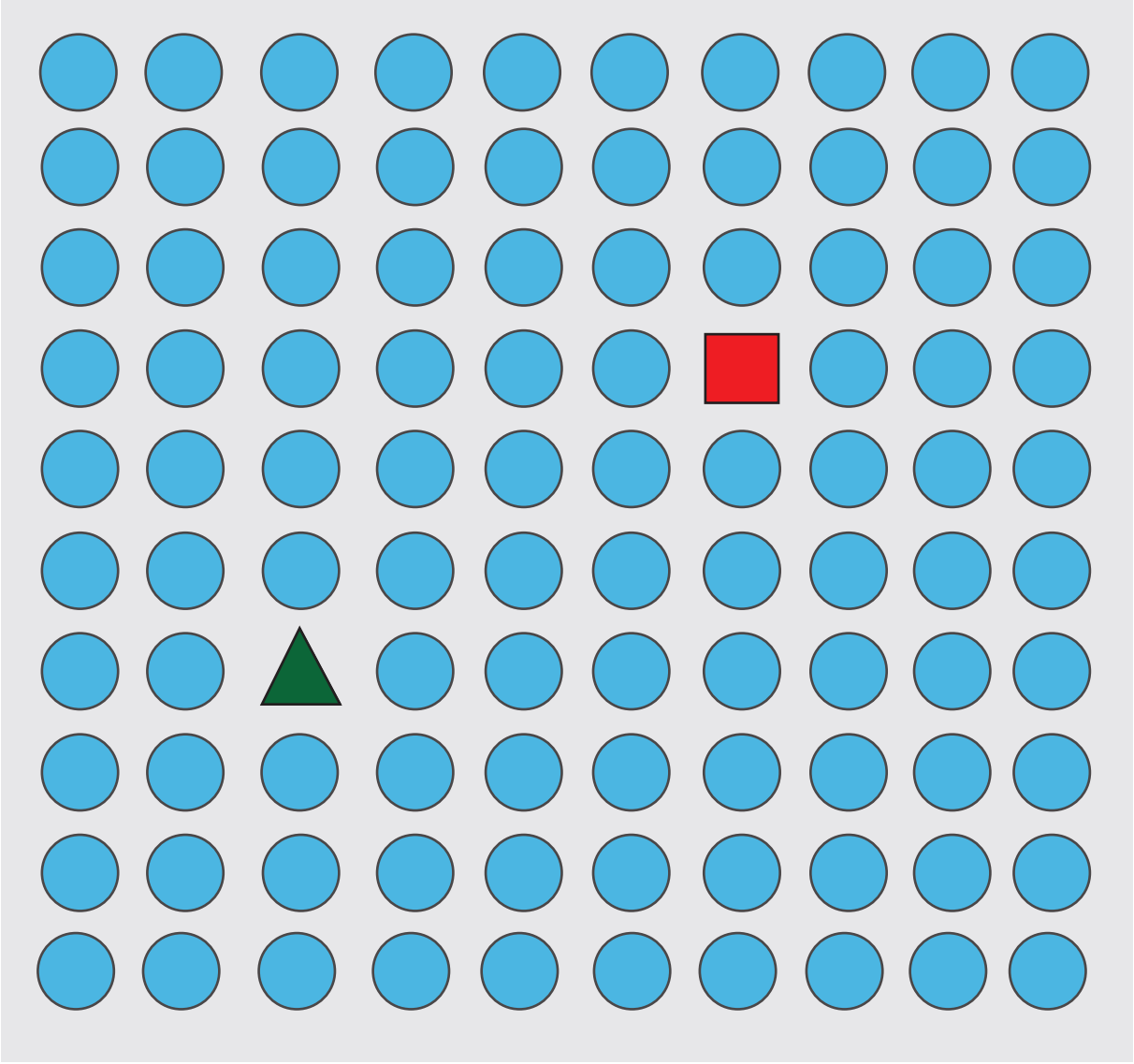

MASTER THESIS

How Cells Count using Social Media:

Study of Density-dependent Effects on Growth and Differentiation of Embryonic Stem Cells

Author:
Pim VAN DEN BERSSELAAR

Supervisor:
Hirad DANESHPOUR

Hyun Youk Group
Bionanoscience Department

August 10, 2018

Abstract

Cells are faced with many decisions. An example is the choice between cell types that cells of the early embryo have to make. Cells from the inner cell mass of mammalian blastocysts can be isolated and cultured to study cell fate decisions *in vitro*. These cells are known as embryonic stem cells (ESCs) and have the ability to self-renew and differentiate into progenitors of the ectoderm, endoderm or mesoderm. To date most studies have focused on unravelling the intracellular regulators and signalling pathways of pluripotency and differentiation. However, it is of interest to understand not how one cell decides on its fate but how a group of those single cells decide on their fate. In this thesis we studied to what extent collective behaviour is involved in groups of mouse ESCs that transit from a pluripotent to differentiated state. By studying the growth dynamics, we found that populations of differentiating mouse ESCs expand, stay stationary or go extinct depending on the seeded density. Aside from controlling growth, the seeded density also controls the differentiation efficiency of the population. Next we aimed to connect the features from the population level with features at a colony level. Analysis of time-lapse microscopy showed that the expansion and extinction of colonies is also density-dependent. Furthermore, the data shows that colonies with a larger initial area and plated at a higher density have a larger probability to survive. Last, we tried to find the molecular mechanism underlying the density dependent population behaviour. Results of a medium transfer experiment hint at a mechanism involving a soluble factor that is secreted into the medium by the cells. RNA-sequencing and RT-qPCR results show that a mechanism involving leukemia inhibitory factor (LIF) is plausible.

Acknowledgements

First I would like to thank Hyun Youk for allowing me to do a project in his group. I also want to thank Hirad Daneshpour for supervising me during my master end project, teaching me everything about stem cells and helping me with my writing and presentation skills throughout the year. Working long days together in the cell culture room with Dua Lipa playing in the background was pretty fun. Many thanks to Stefan who was a bachelor student working on the same project for the first half of my stay. I would also like to thank the rest of the people in the lab, all the scientific and non-scientific discussions during lunch, dinner or a borrel made my time in the lab very enjoyable. Also thanks to Floris for the monthly sunday morning discussions about stem cells. Last I would like to thank Marileen Dogterom and Martin Depken for being members of the thesis committee.

Thanks!

Contents

Abstract **iii**

Acknowledgements **v**

1 Introduction **1**
1.1 Collective Behaviour in Cells . . . 1
1.2 Embryonic Development . . . 2
1.3 Embryonic Stem Cells . . . 4
1.4 Signatures of Collectivity in ESC Populations? . . . 7

2 Materials and Methods **9**
2.1 Cell Culture . . . 9
2.2 Cell Lines . . . 9
2.3 Differentiation Assays . . . 10
2.4 Flow Cytometry . . . 10
2.5 RT-qPCR . . . 11
2.6 Time-lapse Microscopy . . . 12
2.7 Image Analysis . . . 12
2.8 RNA-sequencing . . . 13

3 Results **15**
3.1 Population-level . . . 15
3.1.1 Growth Dynamics . . . 15
3.1.2 Differentiation Dynamics . . . 22
3.2 Colony-level . . . 24
3.3 The Search for a Molecular Mechanism . . . 30
3.4 A Model for Collective Survival . . . 37

4 Discussion **41**

A RT-qPCR **45**
A.1 RT-qPCR amplification program . . . 45
A.2 Primers for RT-qPCR . . . 46

B Additional Results **47**
B.1 Population-level . . . 47
B.2 Colony-level . . . 49
B.3 The Search for a Molecular Mechanism . . . 50
B.4 A Model for Collective Survival . . . 50

C Protocols for maintaining mESCs **51**
C.1 Thawing and Plating mESCs . . . 51
C.2 Passaging mESCs . . . 52

Chapter 1

Introduction

I pass a busy intersection as I ride my bike to the lab every morning. Despite the large number of people at the intersection, traffic flows smoothly. Traffic is organized since everyone follows the same rules; the rules are simple: you go at a green light and you stop at a red light. For the short amount of time spent at the intersection the people's behaviour is almost completely predictable. This behaviour is not restricted to this particular intersection but it is familiar at crossings all over the world. All around us we see groups of autonomous individuals behaving collectively in a way that can be described by a set of simple rules. Traffic is just one example, but there are many spectacular examples of collective behaviour of humans or animals. A flock of birds soaring through the night sky [1]; schools of fish swarming in the ocean to ward off hungry predators [2]; an army of ants building a bridge to reach their spoils [3]; or even cheerful football fans performing a wave to support their country during the world cup (figure 1.1). It sometimes seems like these collective structures have a life on their own, but the individual units have no sense of their location in the overall structure they create. All these collective patterns, such as traffic, look regular and predictable, but it is easy to forget that each individual had a complex reason to be at the intersection at that particular morning. The submergence of the individuals in a global structure arises from local rules which produce global patterns. The whole is greater than the sum of its parts.

1.1 Collective Behaviour in Cells

These global patterns do not only arise at a population level but can also be found at a smaller scale. The human body has levels of organization that build on each other; cells form tissues, tissues form organs and organs form systems. It is cell-to-cell communication that enables groups of cells to form tissues [4]. Cell-to-cell communication is an important factor for the collective behaviour of cells. For collective behaviour of cells one can think of the non-autonomous cell behaviour, *i.e.* any form of coordinated behaviour (growth, decision-making,...). Collective behavior of cells is not restricted to multicellular systems but also occurs in simpler cells such as bacteria. A well studied example of collective behaviour of bacteria is quorum sensing. Quorum sensing is the regulation of gene expression in response to the cell density. In 1970 quorum sensing was observed for the first time in bioluminescent bacteria (*Aliivibrio fischeri*) [5]. At high densities of *A. fischeri* bacteria transcription of luciferase is induced. Luciferase leads to bioluminescence, the production and emission of light by a living organism. These bacteria communicate with each other by secreting and sensing the same molecule, an autoinducer [6]. At a high enough density the local concentration of the autoinducer is higher than a certain threshold

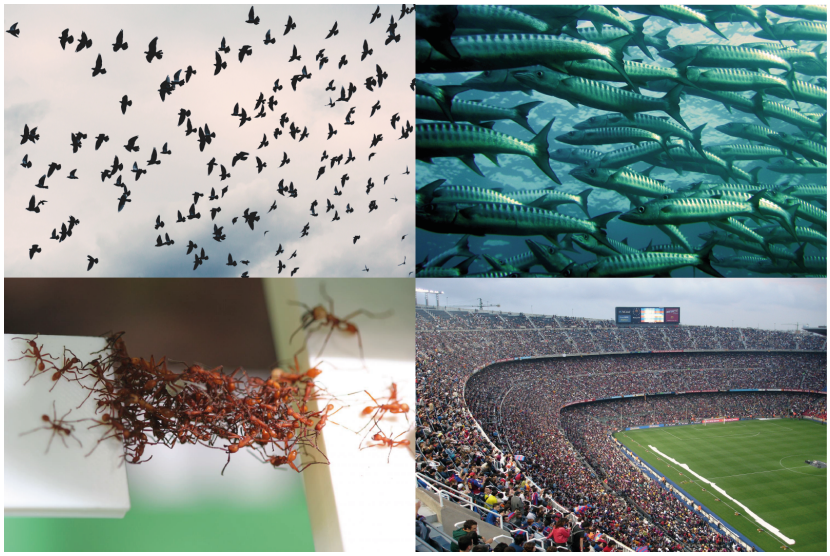

FIGURE 1.1: Examples of collective behaviour. (top left) Flock of birds soaring through the sky (free stock photo). (top right) School of fish (free stock photo). (bottom left) Ants building a bridge (from [3]). (bottom right) Fans cheering on their favourite soccer team (free stock photo).

and the gene expression will alter for the population. Quorum sensing allows for density dependent population behaviour.

Cell-to-cell communication is also involved in the development of an embryo [7, 8]. An embryo that only consists of *e.g.* heart cells would not be much of an embryo, thus cells need a mechanism to know what cell type they need to become during the development process. Pattern formation is one of these mechanism in the embryo and it regulates what identity a cell acquires depending on the cell's relative spatial position in the embryo. Pattern formation itself is regulated by cell signalling [9, 10]. The cells in the early embryo that are able to become any of the three germ lines are termed pluripotent. Coordinated population behaviour has been thoroughly studied in *e.g.* bacteria (quorum sensing), yet we have a poor understanding of the extent to which collective behaviour plays a role in cellular decision-making for these pluripotent cells making up multicellular systems such as humans or mice.

1.2 Embryonic Development

At one point in our lives, we all were just a single cell, yet we ended up as a rather complex living organism. Mice are no different. The development of a single cell into a complex organism is one of many fascinating features of life. In mice the progression of embryonic development is timed by the age of the embryo. The age of the embryo is determined in half-day intervals after mating and is referred to as Embryonic (E) Day. Mouse embryonic development starts with fertilization; a process where a male (haploid sperm cell) and female gamete (haploid egg cell) fuse in the oviduct of the mouse (E0.5). The result of fertilisation is a single diploid cell called the zygote. Succeeding fertilization, the zygote undergoes a succession of divisions with no significant growth, called cleavage divisions. The product is a

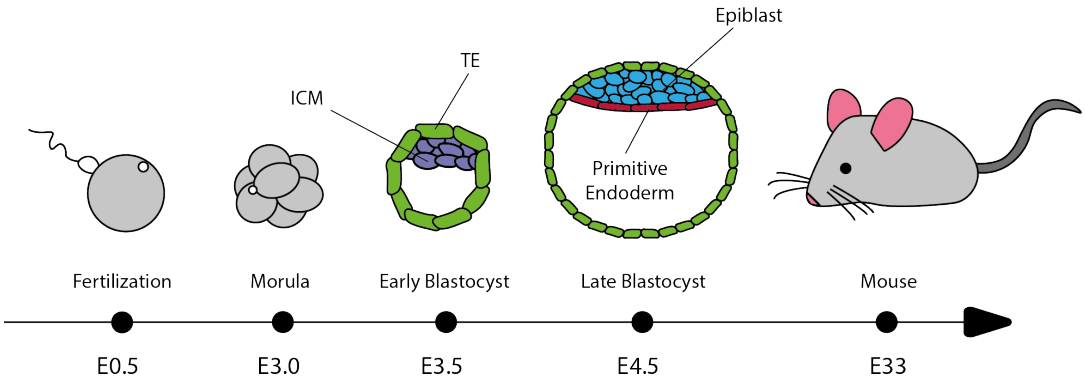

FIGURE 1.2: Simplified schematic overview of different early stages of mouse embryonic development. Time is indicated in days after conception (E). After fertilization (E0.5) the zygote will go through a number of cleavage divisions. At the 8-16 cell stage the cell mass is known as morula (E3.0). Asymmetric cell division of the cells of the morula will results in two different cell types, called trophectoderm (TE) cells and inner cell mass cells (E3.5). These cells form the early blastocyst. The ICM cells will be further segregated into two distinct cell types, the epiblast cells and the primitive endoderm cells (E4.5). At this stage the cell mass is known as the late blastocyst. The late blastocyst will implant into the uterus and eventually develop into a fully functional mouse.

clump of cells that is equal in size as the original zygote. After the fourth cleavage division, the embryo consists of 8-16 cells. At this stage the outer cells become bound tightly together by the formation of intercellular junctions, leading to the formation of a mulberry shaped cell mass known as the morula (E2.5) [11]. This process of deformation is known as compaction. Following compaction, the morula undergoes further cleavages. These cleavages are asymmetric, generating distinct types of outside and inside cell, called trophectoderm (TE) cells and inner cell mass (ICM) cells respectively [12]. Furthermore, the morula develops small intercellular cavities which later unite into one [13]. The trophectoderm cells mediate active transport of ions and the osmosis of water, filling the cavity with fluid and expanding it in the process [14]. The result is a hollow cell-structure with two distinct cell types called the blastocyst (E3.5). The TE cells will later form the placenta, while the ICM is destined to become the embryo. At this stage the cells of the ICM are all pluripotent, *i.e.* they are able to become any cell type that is present in an adult mouse body. By the late blastocyst stage (E4.5), these pluripotent ICM cells will be segregated into two distinct cell types, the primitive endoderm (hypoblast) and the epiblast (primitive ectoderm), the latter cell type will later form the primitive streak [15]. Most of the ICM cells have already decided their fate as either hypoblast or epiblast by E3.5, it was found that ICM cells that express either Gata6 or Nanog at E3.5 will become hypoblast or epiblast cells repsectively [16]. A simplified schematic overview of the early stages of mouse embryonic development is shown in figure 1.2

At E4.5 the late blastocyst implants in the uterus and will consist of roughly 64 cells [17]. Following implantation, is the gastrulation process, which results in the establishment of the basic body plan of the embryo and the formation of the three primary germ layers: ectoderm (*e.g.* cells that become neurons), mesoderm (*e.g.* cells that become heart cells) and endoderm (*e.g.* cells that become lung cells). Gastrulation commences with the formation of an ingression in the posterior region of the

epiblast, the primitive streak. A marker for the primitive streak is the transcription factor Brachyury (T) [18]. Brachyury activates the transcription of genes that are required for differentiation towards the mesendoderm. Epiblast cells move through the primitive streak and will either emerge as a new mesoderm layer or be incorporated into the definitive endoderm [19]. The ectoderm layer is formed by the epiblast cells that do not go through the primitive streak. An early marker for the ectoderm layer commited to a neural fate is Sox1. Sox1 expression induces differentiation towards the neural ectoderm [20]. The exact mechanism behind the formation of the three germ layers and the formation of the primitive streak is not known, however, studies have shown that germ layer development is partly controlled by coordinated cell signalling of the BMP, Activin, Wnt and FGF pathways [21–24]. Aside from ethical issues, the study of signalling pathways in a developing embryo is never an easy job. Luckily, researchers have found a way to study developmental processes *in vitro*.

1.3 Embryonic Stem Cells

In 1981, Evans & Kaufmann and Martin (independently) have isolated the pluripotent ICM cells of the developing mouse blastocyst (E3.5) [25, 26]. When grown as a cell line in tissue culture, these cells are known as mouse embryonic stem cells (ESCs). Stem cells differ from other cell types because they have two unique properties: they have the ability to self-renew and they are pluripotent. Self-renewal is the ability of ESCs to give rise to indefinitely more ESCs, given the culture conditions are right. Self-renewal allows researches to keep an unlimited pool of stem cells at their disposal. Similarly to the pluripotent ICM cells in the embryo, ESCs can give rise to cells from all three germ layers *in vitro*.

Because of these unique properties, stem cells quickly became a crucial tool to study cellular differentiation, the process where a cell changes from one cell type to another, and early embryonic development *in vitro*. Aside from *in vitro* work, Bradley *et al.* have shown that ESCs can also be used to generate chimeric mice [27]. The resulting mice did not only contain chimeric somatic cells, but also contained a chimeric germline, therefore allowing genetic manipulation of mice from culture to creature [28]. A third application of ESCs is in research is in the field of regenerative medicine. At this instance, there are not enough donors of tissues and organs to meet the transplantation demands of the diseased population, leading to a search for alternatives. Stem cells have emerged as the perfect regenerative medicine source because of their two unique properties. In 1998, human embryonic stem cells (hESCs) were isolated for the first time [29]. Human embryonic stem cells can give rise to more than 200 types of cells, so they are a promising treatment for disease. One example of disease treatment is the transplantation of hESCs to patients with spinal cords injuries; implantation improved body control, balance, sensation and limbal movements in patients [30]. Human embryonic stem cells are a promising tool for regenerative medicine, however, ethical concerns limit the application of hESCs. A nobel prize-winning alternative was found in 2006 by Takahashi and Yamanaka. Instead of taking cells from the ICM of a blastocyst, Takahashi *et al.* were able to induce pluripotent stem cells from adult mouse fibroblasts and adult human fibroblasts [31, 32]. Induced pluripotent stem cells (iPSCs) are derived by introducing four transcription factors, Oct3/4, Sox2, c-Myc and Klf4, in adult fibroblasts under cell

culture conditions. These four transcription factors are known as the Yamanaka factors. Inducing pluripotency from adult cells avoids the ethical conflicts associated with using cells from the human embryo (hESCs). Another advantage of iPSCs in regenerative medicine is that the stem cell transplantations are autologous, meaning that the patient uses his own cells and thereby limiting the risk of immune rejection. However, hESCs research also raises some ethical and political controversies. It is favourable to use mESCs, since they are similar to hESCs and the understanding of mESCs is more defined as most previous studies on stem cells have been done on mESCs. In this thesis we use mESCs, since they have an extensive research foundation to build upon. To utilize all of the potential stem cells have to offer, we first need to understand and control how the stem cells differentiate.

One of the first decisions a mouse ESC has to make is whether to differentiate or to stay pluripotent. Maintanance of the pluripotent state is regulated by a group of specific transcription factors. Genetic studies showed that the transcription factor Oct4 is crucial for pluripotency of cells in the ICM *in vivo*, but also for ESCs in an *in vitro* culture [33, 34]. Sox2, a transcription factor that cooperates with Oct4, contributes to the maintenance of pluripotency by regulating Oct4 levels in the embryo and in culture [35, 36]. Sox2 and Oct4 also activate the expression of genes that regulate pluripotency including Nanog. As mentioned in section 1.2, Nanog is expressed in the cells that will eventually form the epiblasts in the ICM. Mitsui *et al.* found that expression of Nanog is also required for the maintenance of pluripotency in epiblasts *in vivo* [37]. Although Nanog has a central role in the maintenance of pluripotency in mouse ESCs, there is evidence that Nanog is not essential for the maintenance of pluripotency, but rather stabilizes the pluripotent state [38, 39]. Together the transcription factors, Oct4, Sox2 and Nanog form the core regulatory circuit that specify embryonic stem cell identity. Oct4, Sox2 and Nanog co-occupy the regulatory regions of their downstream genes, controlling the pluripotent state in a coordinated way [40, 41]. The proteins of the core regulatory circuit also control their own expression and each other's expression with both positive and negative feedback regulation [42, 43].

The state of ESC pluripotency is not solely controlled by these transcription factors but pluripotency is also under cell-extrinsic control. Leukemia inhibitory factor (LIF) is a signalling factor that mainly blocks differentiation of mouse ESCs in *in vitro* cultures, although LIF is not necessary for the maintenance of pluripotency in the ICM *in vivo* and *in vitro* [44, 45]. LIF binds to a receptor heterodimer consisting of LIF receptor (Lifr) and Gp130, activating the JAK/STAT3 signalling pathway [46]. Aside from the JAK/STAT3 pathway, LIF also activates the PI3K and the mitogen-activated protein kinase (MAPK) pathways [47, 48]. The downstream target of JAK/STAT3 pathway is c-Myc, one of the Yamanaka factors that can induce pluripotency [49]. However, MAPK signalling promotes differentiation [50]. Since a low level of MAPK signalling is crucial for the maintenance of pluripotency, ESCs are often grown in media in which in addition to LIF, chemical inhibitors of differentiation are added to keep the cells in a pluripotent state. Another signalling pathway also play an important role in the maintenance of pluripotency in ESCs. Bone morphogenetic proteins (BMPs) that signal through SMAD proteins, promote the expression of differentiation inhibitors [51]. To keep mouse ESCs in a pluripotent state *in vitro*, cells are grown in either a serum based medium in which differentiation is blocked by LIF and BMP (BMP cytokines are present in serum) or a medium in which differentiation is blocked by the combination of LIF and 2 chemical inhibitors

(PD0325901 a MAPK inhibitor (PD03) and CHIR99021 a Wnt agonist (CHIR)). To sustain in a pluripotent state, stem cells express transcription factor that promote pluripotency and activate pathways that inhibit differentiation as shown in figure 1.3.

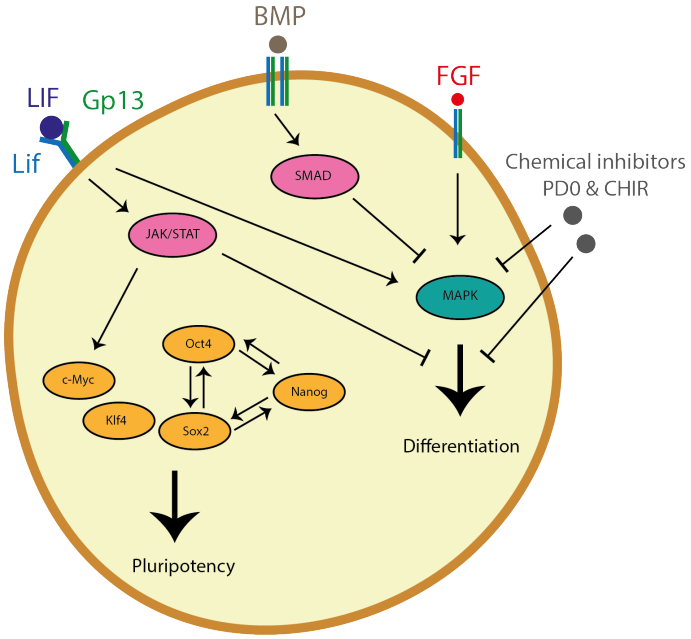

FIGURE 1.3: Simplified schematic overview of pluripotent maintenance in mouse embryonic stem cells. LIF simultaneously activates the JAK/STAT3 pathway, which promotes pluripotency maintenance, and the MAPK pathway, which promotes differentiation. *In vitro* differentiation is blocked by the activation of the BMP pathway or by the addition of two chemical inhibitors. The onset of differentiation is a result from the activation of the FGF pathway and the withdrawal of the factors that induce pluripotency and inhibit differentiation.

By changing the culture condition (removal of LIF and serum or the chemical inhibitors), mouse ESCs leave the pluripotent state and differentiate into one of two lineages: progenitors of the mesendoderm (ME) or progenitors of the neural ectoderm (NE). Differentiation is initiated by the stimulation of the MAPK signalling pathway by fibroblast growth factors (FGFs) [52, 53]. Following initiation, the cell has to choose whether to differentiate towards the ME lineage of the NE lineage. This choice depends on the signalling environment around the cell. Activation or inhibition of the BMP, Activin, Wnt and FGF pathways can guide cells to one of either lineages. Progenitors of the ME *in vitro* resemble the cells of the primitive streak in a developing embryo. Like the primitive streak *in vivo*, stem cells differentiating toward the ME start expressing Brachyury, the earliest marker of mesendoderm differentation [54]. ME differentiation is initiated by activation of the Activin or Wnt pathways [54–56]. This knowledge gave researchers a way to guide differentiation *in vitro* by adding signalling molecules that activate the Activin or Wnt pathways to the medium such as the previously mentioned CHIR chemical inhibitor. In combination with PD0, CHIR serves as a differentiation inhibitor, however, by itself CHIR promotes the Wnt pathway which promotes ME differentiation. Like Brachyury in ME, differentiation towards the NE lineage is characterized by expression of Sox1 [57].

Ying *et al.* found that inhibition of the BMP, Activin and Wnt together with an activation of the FGF pathway result in the differentation of mouse ESCs towards the NE fate [58,59]. The NE lineage is often considered the default pathway, as mouse ESCs will differentiate towards the NE when no serum or ME inducers are present. Even though it is considered the default pathway, research use retinoic acid (RA) to enhances NE differentiation in cell cultures. RA speeds up differentiation towards the NE-lineage by regulating the FGF pathway [60]. An overview of the first differentiation step of mouse ESCs is shown in figure 1.4. Aside from the signalling pathways, the up- and down-regulation of the pluripotency factors Oct4 and Sox2 also are key in the differentiation process [61]. Expression of Oct4 inhibits NE differentiation and promotes ME differentiation. On the contrary Sox2 promotes NE differentiation and suppresses ME differentiation.

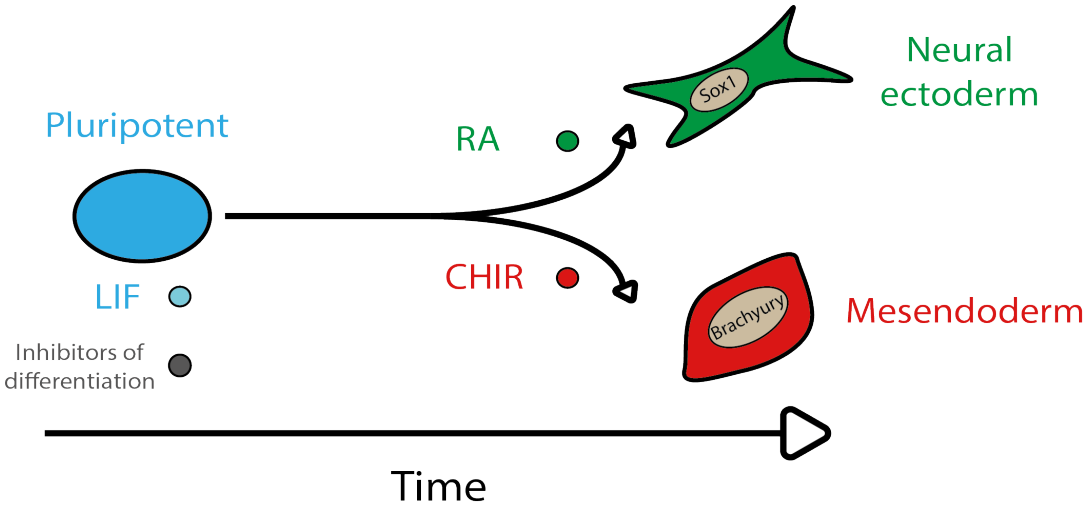

FIGURE 1.4: Overview of the first differentiation step of mouse embryonic stem cells. ESCs are kept in a pluripotent state by the signalling molecule LIF and inhibitors of differentiation (*i.e.* PD0,CHIR,serum). Removal of these factors starts the differentiation process. Differentiation towards the neural ectoderm (NE) is promoted by the addition of retinoic acid (RA). Differentiation towards the mesendoderm (ME) lineage is promoted by the addition of CHIR99021 (CHIR).

Although the pathways that govern differentiation have been thourougly studied, controlling differentiation remains a difficult process. Researchers have not established a protocol yet in which they were able to differentiate the cells homogeneously with a purity of 100 percent [51]. To add to the confusion, the Wnt pathway has also been found important in the maintanence of pluripotency and differentiation towards the NE lineage [62,63]. How all the pathways are interconnected during the differentiation process remains a mystery for now. Perhaps the view of a linear pathway in single cells is not complete, approaching differentiation from a systems biology point of view might result in more insights in the field.

1.4 Signatures of Collectivity in ESC Populations?

From the development of an embryo we know that stem cells are more than just complex individuals. Throughout embryonic development, cells have to coordinate their behaviour and cell fate to grow into a functional embryo. To date focus in ESC research has primarily been on unravelling intracellular regulators of pluripotency and differentiation, and response behaviour of ESCs to extracellular signalling molecules often presented into the cell culture medium by the experimentalist. Moreover, it is of significant interest to understand not how a single cell decides on its fate but how a group of those single cells decide on their fate. Individual ESCs within a population (in an embryo or on a dish) may likely affect each others decisions by natively secreting and sensing signalling molecules, hence establishing cell-to-cell communication. A better understanding of how population-level behaviours emerge from single cell-level dynamics would be beneficial for the stem cell field, as it provides manipulative rules governing the stem cell behaviour (e.g. improving differentiation and reprogramming efficiencies). From previous research we know that cell-to-cell signalling plays a role in the maintenance of pluripotency and the differentiation process. In this thesis I have contributed to a work addressing to what extent collective behaviour is involved in groups of cells that transit from a pluripotent to a differentiated state. In particular, we asked how embryonic stem cells coordinate their behaviour within a differentiating population.

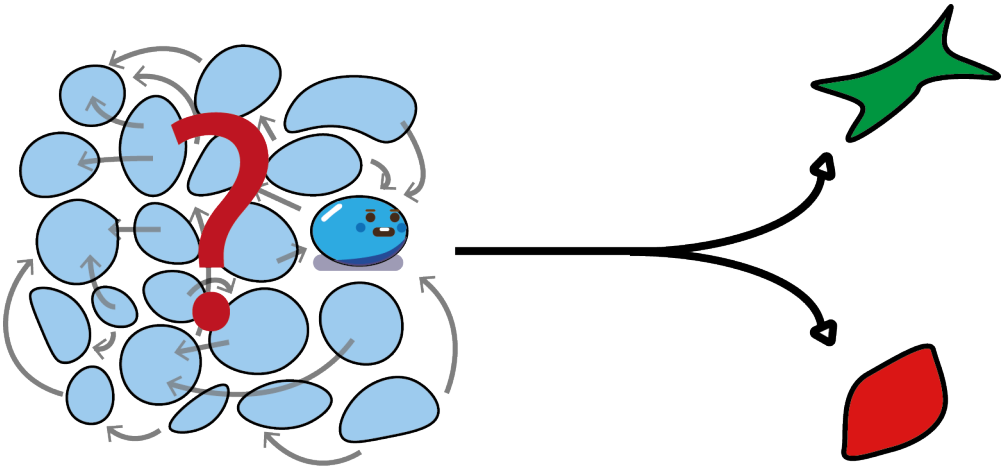

FIGURE 1.5: Illustration of the research question adressed in this thesis.

Chapter 2

Materials and Methods

2.1 Cell Culture

Mouse ESCs were routinely propagated in LIF-supplemented medium on 0.1% gelatin coated dishes (Sarsted $\varnothing 10cm^2$). Two types of media were used to keep the cells in a pluripotent state, serum/LIF (S+L) medium and N2B27+2i+LIF (2i+L) medium. Serum/LIF medium consists of the basal medium dulbecco's modified eagle's medium (DMEM, Gibco) with 15% Fetal Bovine Serum (Gibco). This medium is supplemented with 1% Non-essential amino acids, Sodium Pyruvate and GlutaMAX (all Gibco 100x), 0.055 mM 2-β mercaptoethanol and $10^3 \frac{U}{ml}$ LIF.

N2B27 medium, as described in Ying *et al.*, is a mixture of nearly 1:1 DMEM/F12 +GlutaMAX (Gibco) and Neuralbasal (Gibco) supplemented with 0.5% Non-essential amino acids, Sodium Pyruvate, GlutaMAX and N2 (all Gibco 100x), 1% B27-Vitamin A (Gibco 50x), 0.055 mM 2-mercaptoethanol, and 8.3 μg BSA [59]. Addition of $10^3 \frac{U}{ml}$ LIF, 0.008mM CHIR99021 and 0.0025mM PD0325901 to N2B27 will keep the cells in a pluripotent state. In combination, the two chemical inhibitors PD0325901 and CHIR99021 with LIF maintain the pluripotent state of mouse ESCs [50].

Cells were passaged using accutase (Gibco), a cell detachment agent, and replated every two or three days with a split ratio of 1 in 10. Cells were kept in an incubator at 37° at 5% CO_2 (Eppendorf). Accutase was preferred over the commonly used cell detachment agent trypsin, which is more harsh for the cells.

2.2 Cell Lines

Cell lines used in this thesis were E14Tg2a, 46C, Brachyury-GFP, E14/N14 and Oct4-GFP. The E14Tg2a (E14) wild type cell line was originally derived from the mouse strain 129/Ola by Martin Hooper [64]. 46C is a modified E14Tg2a cell line in which the open reading frame of one copy of Sox1 has been replaced with GFP [59]. Brachyury-GFP ESC line is an E14Tg2a carrying a GFP reporter cassette knocked in the Brachyury locus [65]. E14/N14 is derived from E14Tg2a and contains a GFP reporter in the Nanog locus. Similar to Brachyury and E14/N14, the Oct4-GFP report cell line has a GFP report knocked in the Oct4 locus.

The cell lines, E14Tg2a, 46C and Brachyury-GFP were maintained in Serum/LIF medium; E14/N14 and Oct4-GFP were maintained in N2B27+2i/LIF unless stated

otherwise, as propagation of Oct4-GFP and E14/N14 in S+L resulted in unhealthy looking cells and visible pre-differentiation. S+L was chosen for pluripotency maintenance, since this is standard in the field.

2.3 Differentiation Assays

Differentiation assays were adapted from established NE and ME differentiation procedures [59]. In the differentiation assays described here allow differentiation towards the ME or NE by adding one single molecule to the cell culture medium. Mouse ESCs were accutased, washed and replated into N2B27 medium at the desired density. After 48 hours, cells can be affected by signalling so the old medium was replaced with fresh N2B27 with a single molecule that drives differentiation towards the ME or NE lineage [61]. For NE differentiation retionoic acid (RA), a regulator of the FGF pathway (see section 1.3), was added. For ME differentiation CHIR99021, a Wnt agonist, was added [66]. After x amount of days, depending on the experiment, cells are accutased and the number of cells is determined by a hemocytometer. Fluorescence is measured using flow cytometry.

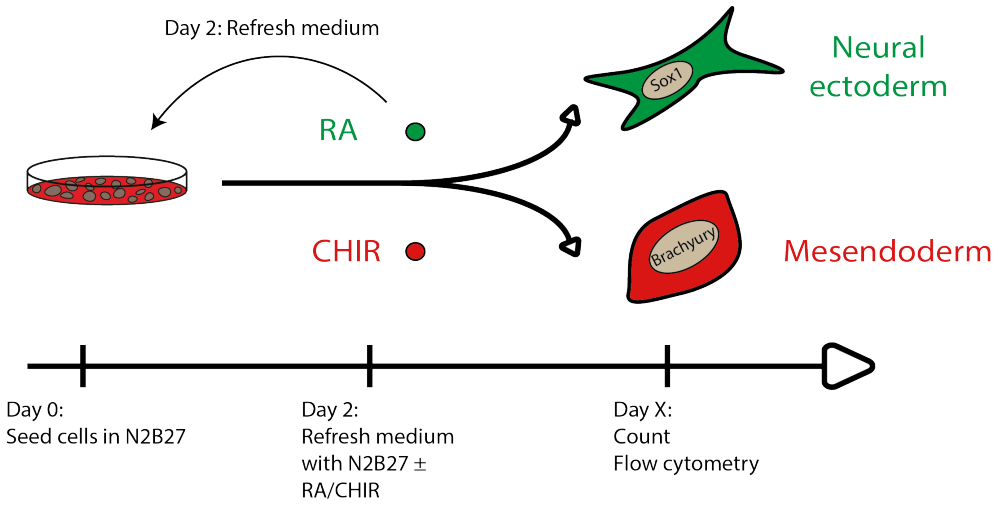

FIGURE 2.1: In a differentiation assay, cells are seeded at the desired density in N2B27. Two days after plating the medium is refreshed with N2B27 and a signalling molecule that drives differentiation. For neural ectoderm (NE) differentiation, retionoic acid (RA) is added. For mesendoderm (ME) differentiation, CHIR99021 (CHIR) is added. On day x (x=1,2,3,4,5,6,.....) cells are counted and fluorescence is measured.

2.4 Flow Cytometry

Flow cytometry was performed with a BD FACSCelesta equipped with blue (488-nm), yellow-green (561 nm) and violet(405-nm) lasers. Based on the forward and side scatter, living cells are separated from dead cells and noise. The forward scatter reports the relative size of the cell. The side scatter reports the complexity or granularity of the cell. Sorting gate for GFP positive and negative populations is

set by comparing signals of differentiated and pluripotent cells, *e.g* by comparing the Sox1:GFP signal in a pluripotent population (signal off) to a NE differentiated population (signal on) a proper gate could be constructed (see figure 2.2 (B)). In differentiation experiments we report the percentage of cells that fall within this gate. Data was further analysed using FlowJo software. For very low cell numbers, flow cytometry was used as a cell counter. A control experiment in which we measured medium that was kept on a plate without cells for six days showed that noise in measurements will not interfere with the count numbers.

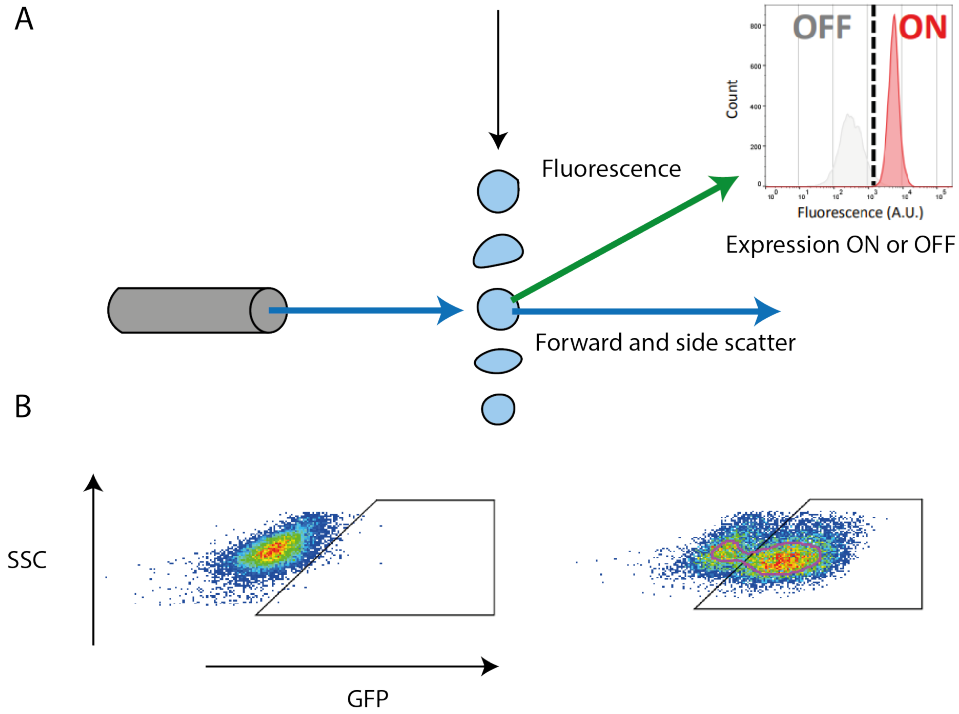

FIGURE 2.2: (A) Schematic overview of flow cytometry. When cells flow through the cytometer, the forward,side-scatter and fluorescence of the cells are measured. These measurements are then used to generate a plot of the population profile for these parameters. (B) Construction of a gate to distinguish GFP on from GFP off cells. On the left side all the cells are GFP off. On the right a fraction of the population turned GFP on.

2.5 RT-qPCR

For reverse transcriptase quantitative PCR (RT-qPCR) experiments cells were accutased and washed twice in PBS after the desired amount of days. RNA was isolated using Purelink RNA mini kit (ambion), with the additional step of DNAse treatment (Qiagen). Reverse transcription was performed using iScript cDNA synthesis (Bio-Rad). QPCR was performed in three technical replicates on Illumina's EcoTM Real-Time PCR System using SYBR Green Supermix (Bio-Rad). The obtained gene expressions were normalized using a reference housekeeping gene GAPDH. The fold enrichment was calculated by using the $2^{\Delta\Delta Ct}$ method ([67]), where $\Delta\Delta$Ct = ΔCt(normalized sample) – ΔCt(normalized day 0). The primers and temperature protocol used for the qPCR can be found in the appendix.

2.6 Time-lapse Microscopy

For live cell microscopy, cells were plated at the desired density on a 0.1% gelatin coated $\varnothing 6cm$ culture dish in N2B27 medium. Cells were imaged using the SMZ25 stereo microscope (Nikon). During the imaging process cells were kept in an environmental chamber incubator that was kept at 37° C and 5% CO_2. Brightfield images were aquired every hour for a period of 96 hours with an exposure time of 300ms and 90x magnification with an 1x objective. For each field of view five Z slices were acquired. The microscopy data was analysed using custom MATLAB software.

2.7 Image Analysis

Home made semi-automatic segmentation software was used to analyse the microscopy data. Cells were segmented by a threshold method in which the deviation of pixel values compared to the mean pixel value was calculated per cell. Since the edges of the cell have the highest deviation from the mean, cells could be accurately segmented by thresholding. In the last step noise is removed and the segmented edges of the colony were filled. From the segmented colonies, the area parameter was retrieved.

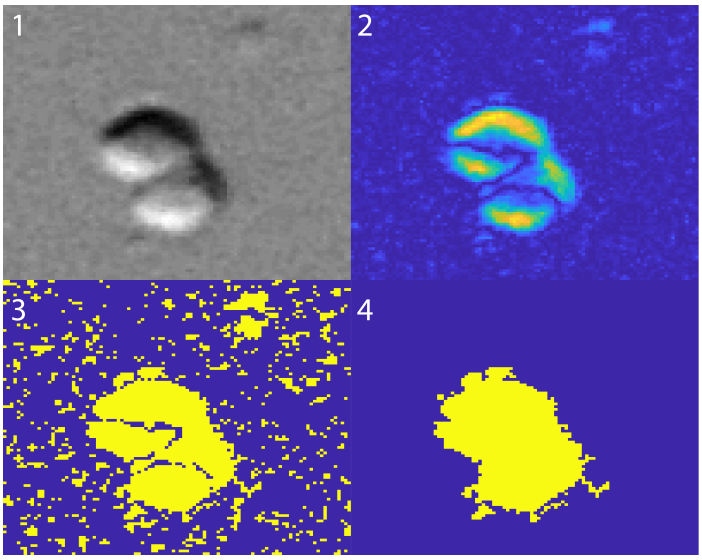

FIGURE 2.3: Overview of the segmentation process. (1) The brightfield image of original colony. (2) The deviation of all the pixel values compared to the mean. (3) The threshold binary image of the colony. (4) Noise was removed and the edges of the colony were filled.

2.8 RNA-sequencing

RNA-sequencing was performed by Hirad Daneshpour. For sequencing the RNA of E14 cells was extracted as described in the RT-qPCR section. cDNA library was prepared using the Lexogen QuantSeq FWD 3′ mRNA-Seq Library Prep Kit. Sequencing was performed with a Illumina MiSeq Personal Sequencer. Tuxedo Suite was used for the read alignment. Tuxedo Suite contains the open source software tools Bowtie, TopHat and Cufflinks [68–70]. These tools enables comprehensive analysis of RNA-sequencing data. Reads were normalized and expression level is reported in fragments per kilobase of transcript per million mapped fragments (FPKM).

Chapter 3

Results

We know that ESCs have the molecular tools to communicate with each other (*e.g.* through Fgf, Bmp, Wnt, Notch-delta signalling). As cell-to-cell communication is often mediated through extracellularly secreted diffusible molecules or through cell contact-dependent signalling, most likely altering the seeded number of cells will affect the strength of communication as it varies the space between cells/colonies. We start by studying the effect of altering the seeded number of cells at a population level. By zooming in to a colony level, more insights into how collectivity is established could be found. The last step would be to determine the molecular mechanism behind collectivity in differentiating ESC populations. In addition, a preliminary model based on the reaction-diffusion equation is provided to potentially give more insights into the system.

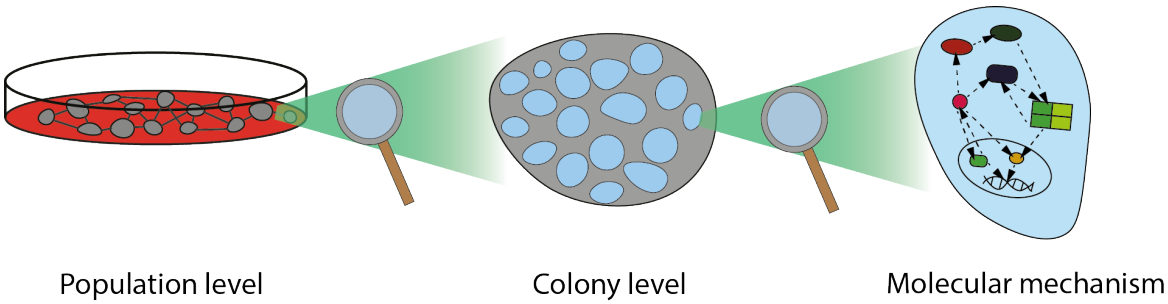

FIGURE 3.1: Overview of results chapters covered in this thesis. Starting at a population level and slowly zooming in to a molecular level.

3.1 Population-level

3.1.1 Growth Dynamics

We started studying the growth of pluripotent and differentiating ESCs by only altering the seeded number of cells N_{seeded}. ESCs were grown for six days on a $\varnothing 10cm$ plate in different types of media, refreshing the cell culture media on day two.

In figure 3.2, we see that when cells are grown in a pluripotency medium, *i.e.* Serum/LIF (S+L) or N2B27+2i+LIF (2i+L) (purple and dark blue respectively), cells will grow and survive irrespective of the seeded number of cells. Interestingly, when grown in a differentiation medium such as N2B27 with or without retinoic

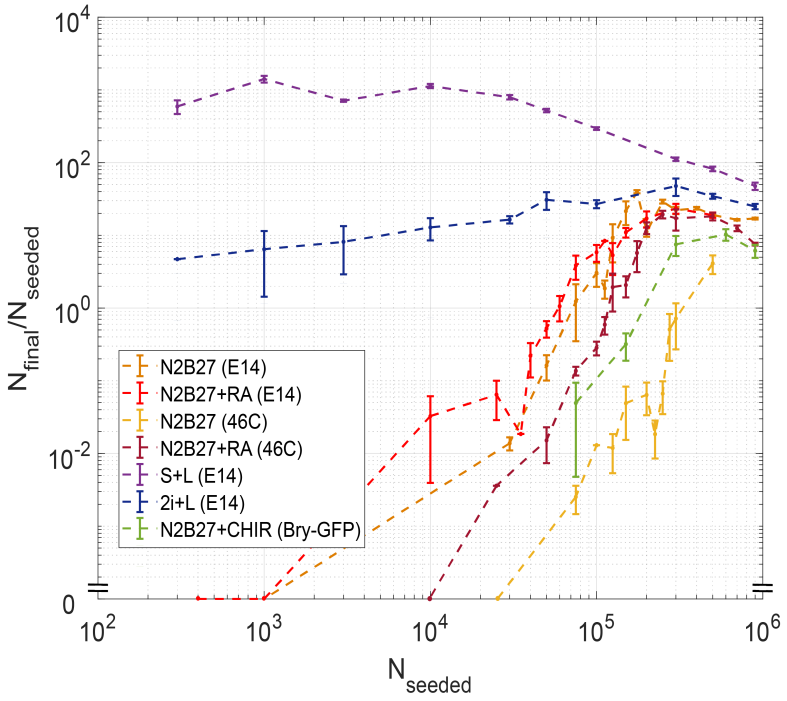

FIGURE 3.2: Plot of growth ($\frac{N_{final}}{N_{seeded}}$) versus the seeded number of cells N_{seeded}. Cells were plated on a $\varnothing 10cm$ dish in different types of media, the media was refreshed on day two. Six days after plating N_{final} was measured using a hemocytometer. Colours represent the different conditions and cell lines. Both pluripotency (S+L (serum LIF), 2i+L (N2B27+2i/LIF) and differentation (N2B27 $\pm$ retionoic acid(RA)/CHIR99021(CHIR)) media were used. The addition of RA or CHIR to the medium guided differentiation towards the neural ectoderm (NE) or mesendoderm (ME) lineage respectively. Error bars represent the standard error of the mean of a minimum of three biological replicates.

acid or CHIR99021 (N2B27 $\pm$ RA, N2B27 $\pm$ CHIR respectively), cells plated at low seeded densities show an extinction trend over the course of 6 days, while cells at high seeded densities survive and grow similarly to the cells in a pluripotent state. These results indicate that the survival of differentiating cells is density dependent. Another feature is the sharp transition from dying to expanding differentiating cell populations. A 10-fold change in N_{seeded} results in 100 fold change in growth (N_{final}/N_{seeded}) for E14 cells grown in N2B27+RA. In comparison, when cells are grown in a pluripotency medium a 10 fold change in N_{seeded} results in a 5 fold change in N_{final}/N_{seeded}. Experiments were done both in the wildtype (E14) (orange and red) and 46C (brown and yellow) cell lines as a control to test that the transition was not cell line dependent. Similarly, a control with (red and purple) and without (orange and yellow) RA and CHIR (green) was carried out. Both controls show that the transition is not dependent on the cell line or the signalling molecules RA and CHIR. Also, these controls show that it does not depend whether cells differentiate towards the NE or ME lineage. The last minor feature these results show is that cells that have been exposed to RA tend to grow better than the cells that have not, *e.g* compare value of N_{final}/N_{seeded} of N2B27 (46C) (yellow) to value of N_{final}/N_{seeded} N2B27 + RA (46C) (brown) at $N_{seeded} = 10^5$.

These findings show that the population growth dynamics of differentiating ESCs is not straightforward, *i.e.* the seeded number of cells determines whether the population can expand and therefore reach the carrying capacity of the plate. Cells plated at a low number of seeded cells have more available space to grow and more nutrients available per cell than the cells plated at a high number of seeded cells. Also, ESCs in a pluripotent state grown in N2B27+2i+LIF are able to survive irrespective of the number of seeded cells, while cells grown in just N2B27 die over time at a low number of seeded cells. As we observed that the seeded population either expands or goes extinct, we can conclude that there is a population-level control for growth exclusively during differentiation.

Next, we wondered how the sharp growth transition emerged in time. For the experiments, cells were grown over a period of up to 15 days in N2B27 medium which was refreshed with N2B27 + RA on day two. These experiments were done with both the E14 and 46C cell lines.

Overall, E14 (3.3 (A)) shows similar growth characteristics as 46C (3.3 (B)). Cells plated at a high number of seeded cells expand, while cells at a low number of seeded cells number show an extinction profile. Shown in figure 3.4 are the microscopy snapshots that complement that data. In the top panel a high seeded number of cells was plated on a $\varnothing 10cm$ dish ($N_{seeded} = 300k$, $k = 1000$), in the bottom panel a low seeded number of cells was plated ($N_{seeded} = 75k$). Snapshots were taken of day one, day three and day five of the 46C cell line. The snapshots show that the morphology of the colonies changes drastically over a short period of time. The morphology changes from a packed shape (with rather spherical cells) to a spiky shape (with rather flat cells) which is a characteristic of NE differentiation [59]. The snapshots also show the occurrence of some cell dead for cells plated at a high seeding density.

The data in figure 3.3 shows a third interesting feature. For both the E14 ($N_{seeded} = 75k, N_{seeded} = 70k, N_{seeded} = 60k$) and 46C ($N_{seeded} = 112k, N_{seeded} = 100k$) cell lines, there is a certain range of initial densities in which the population neither expands nor goes extinct. We refer to this feature as the stationary population. The stationary population is not an artefact of a particular cell line, since it appears in both the wild type and modified cell lines.

Figure 3.5 is another representation of figure 3.3 (B) for a set of N_{seeded}. Figure 3.5 clearly demonstrates the narrow range of seeding densities for which the stationary populations occurs. Less than a two fold difference in seeded number of cells in this range can make the difference between an expanding or dying population, $N_{seeded} = 100k$ is a stationary population, $N_{seeded} = 200k$ is an expanding population and $N_{seeded} = 50k$ is a population with an extinction trend. These results hint that the transition from a population expanding or going extinct is critical, *i.e.* there is a critical threshold of seeded number of cells which dictates the tipping point of the populating expanding or going extinct. Interestingly, there is a range ($[N_{seeded} = 125k, N_{seeded} = 75k]$) around this threshold for which the population remains stationary in the course of six days.

These critical transitions can also occur in natural populations of fish. Small environmental perturbations can wipe out a whole population if near a critical threshold. A plausible example is the collapse of the Canadian cod fishery in Nova Scotia [71].

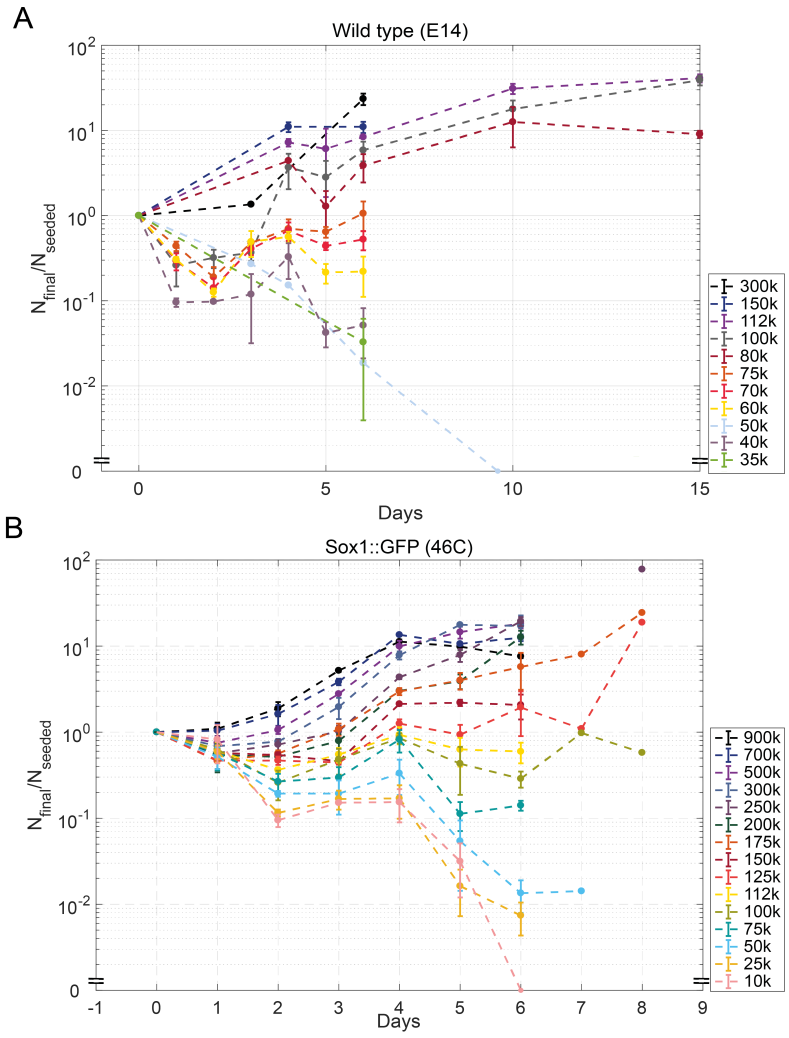

FIGURE 3.3: Growth dynamics over a timespan of up to fifteen days for E14 (A) and 46C (B) cell lines. Cells were grown on a $\varnothing 10cm$ dish in N2B27 medium which was refreshed with N2B27 + RA on day 2. N_{final} was measured using a hemocytometer. The legend represent the initial number of seeded cells with $k = 1000$, colours do not match between (A) and (B). Error bars represent standard error of the mean of a minimum of three biological replicates.

An explanation for such a collapse is that the growth rate at low population densities is negative and maximum at intermediate densities, this biological phenomenon is known as the strong Allee effect [72] (inline 3.6). The Allee effect is observed in many species and influences the dynamics of a population. The proliferation rate at the higher population number reduces because of *e.g.* a shortage of space and nutrients. The curve crosses the $\frac{dN}{dt} = 0$ at K, the carrying capacity of the population, at 0, where the population has gone extinct, and at a third point in between. The strong Allee can be modelled mathematically by a differential equation:

$$\frac{dN}{dt} = rN(\frac{N}{A} - 1)(1 - \frac{N}{K})$$

where N is the population size, r the growth rate, K the carrying capacity and A the critical point.

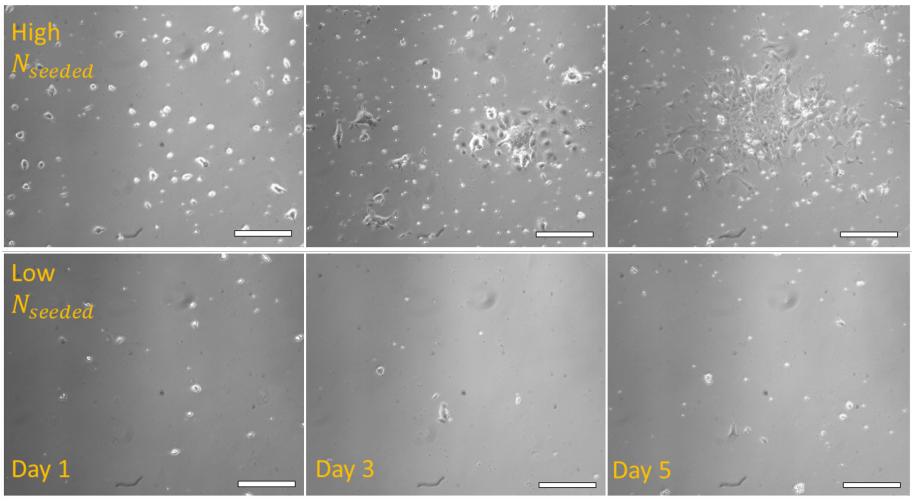

FIGURE 3.4: Microscopy snapshots of 46C cells at $N_{seeded} = 300k$ (top) and $N_{seeded} = 75k$ (bottom) from day one, day three and day five after seeding the cells (left to right). Cells were grown on a $\varnothing 10cm$ dish in N2B27 medium which was refreshed with N2B27 + RA on day two. The "blur" in the images from the high N_{seeded} due to many floating dead cells. Scale bar = 200 μm

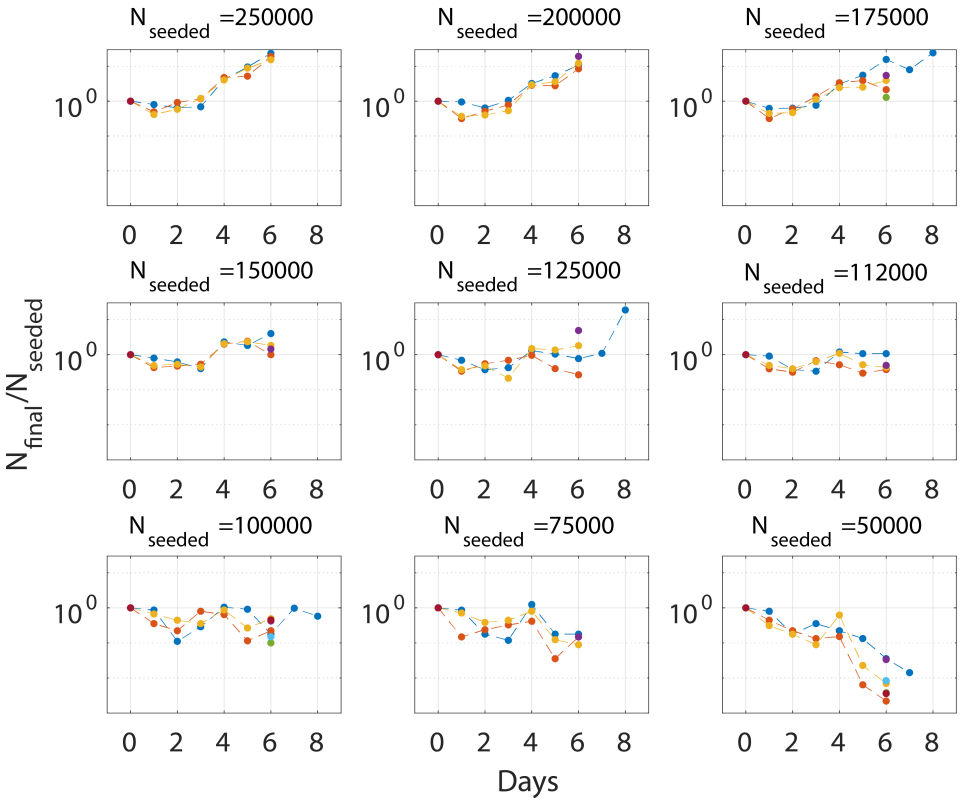

FIGURE 3.5: Growth dynamics over a timespan of six days of 46C cells at nine different seeded cell numbers N_{seeded}. Cells were grown on a $\varnothing 10cm$ dish in N2B27 medium which was refreshed with N2B27 + RA on day two. N_{final} was measured using a hemocytometer. Different colours represent the different biological replicates.

We find signatures of the strong Allee effect by re-plotting data shown in figure 3.3 (B). Analysing the change of population number over subsequent days as function of the number of cells at time t allowed to identify the fixed points of the system (figure 3.6). For this system, the fixed points are identified at the points at which the ratio of population numbers between subsequent days $\frac{N_{t+1}}{N_t}$ is equal to one, with N_t the population number at day t (t=1 to 6). These fixed points resemble the conditions at which there is no change in population size over time. If we assume the strong Allee effect to be present in the system we can find the seeding densities corresponding to the fixed points by least mean square fitting the mathematical model of the Allee effect to the data. The stability of the fixed points is determined by whether the population will return to the fixed points if the population number is perturbed around the fixed points or not. The fixed point at $N_t \approx 10^7$ is stable, this point is located at the carrying capacity K of the dynamical system. A population larger than the carrying capacity has a growth (N_{t+1}/N_t) smaller than one, such that the population will shrink to the carrying capacity. However, a population smaller than the carrying capacity and larger than the other fixed point will have a growth larger than one, such that the population will grow to the carrying capacity. The other fixed point located at the critical threshold at $N_t \approx 5.5 \cdot 10^4$ is unstable. Populations larger than the critical threshold will grow towards the carrying capacity and populations smaller than the critical threshold will go extinct. At the critical threshold a small perturbation in the seeded cell number can shift the growth behaviour of the population (extinction or expansion of the differentiating ESC population) to a different one. Seeding cells below the critical threshold reveals a loss of resilience during differentiation compared to when maintained pluripotent. The third fixed point (stable) of the system is located at $N_t = 0$ (not shown in figure 3.6).

Generally in dynamical systems, the rate at which the system recovers from a small perturbation close to the critical threshold is very low, this phenomenon is known as critical slowing down [73]. For the case of differentiating ESCs it would mean that when cells are plated at a N_{seeded} closer to the critical threshold, the population needs longer to reach stable state. In general, as you get closer to critical threshold, the time needed to reach the stable state will go to infinity. Some indicators of critical slowing down are an increase in variation and autocorrelation time in population number close to the critical threshold. A preliminary experiment in which eight plates of $N_{seeded} = 100k$ of 46C cells were grown in N2B27 and refreshed with N2B27+RA on day two for a period of 15 days, show that the populations of three out of eight plates survive and the remainder populations die after 15 days (illustrated in figure 3.7). In figure 3.7 growth dynamics from figure 3.3 (B) for $N_{seeded} = 500k$, $N_{seeded} = 100k$ and $N_{seeded} = 50k$ are shown for reference. Plotting the variation of population number after 15 days of growth for these three conditions would result in the largest variation for $N_{seeded} = 100k$. Although, experiments in which plates with $N_{seeded} = 500k$ and $N_{seeded} = 50k$ are grown for 15 days are still lacking as mentioned in the discussion. However, these results already indicate that there is critical slowing down at the critical threshold of the system of differentiating cells. This critical threshold would imply that the differentiating ESCs are a homogeneous connected network on a plate [74]. These results are an early sign of population-level collectivity of ESCs committing to the NE or ME lineage.

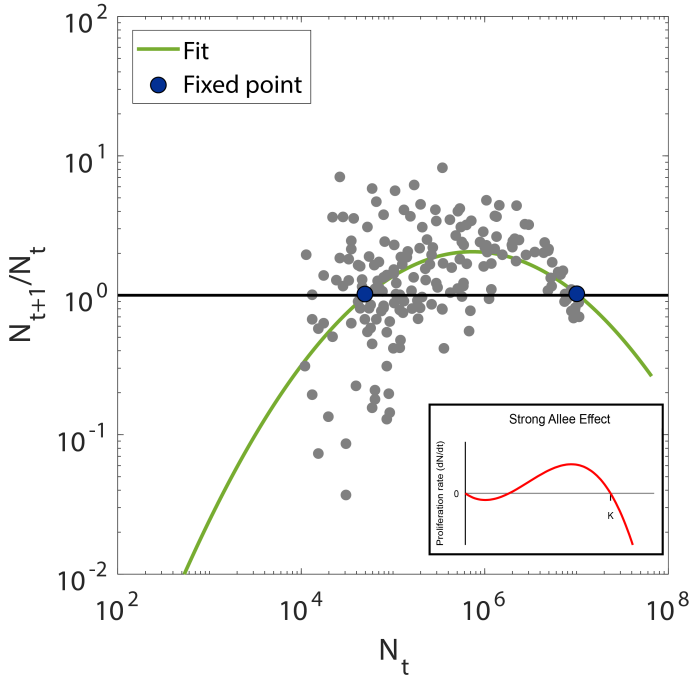

FIGURE 3.6: Analysis of the change of population number over subsequent days (t = 1 to 6) as function of the seeded number of 46C cells (grey data points). Cells were grown on a $\varnothing 10cm$ dish in N2B27 medium which was refreshed with N2B27 + RA on day two. N_y was measured using a hemocytometer. A least mean square fit (green) through the data points was based on the mathematical description of the strong Allee effect (inline). The fixed points (blue) are identified at $\frac{N_{t+1}}{N_t} = 1$.)

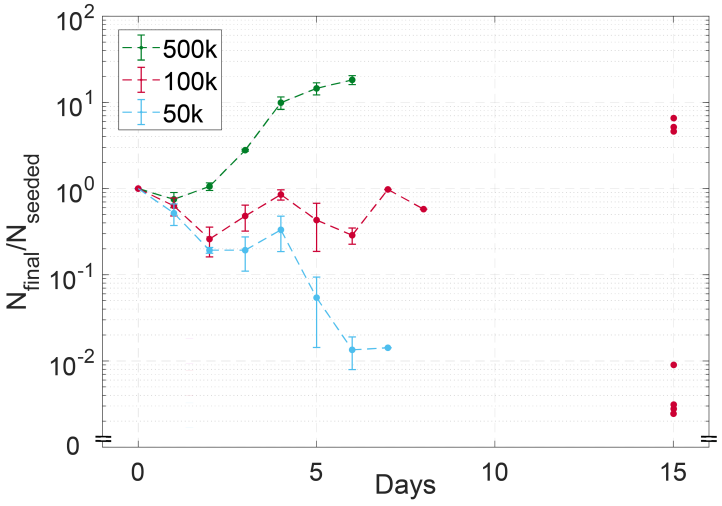

FIGURE 3.7: Growth dynamics over a timespan of up to 15 days of 46C cells at three different seeded cell numbers N_{seeded}. Cells were grown on a $\varnothing 10cm$ dish in N2B27 medium which was refreshed with N2B27 + RA on day two. N_{final} was measured using a hemocytometer. Different colours represent the different seeded number of cells. Errorbars indicate standard error of the mean.

In summary, a population of differentiating ESCs expands, stays stationary or goes extinct depending on the seeded number of cells. These features indicate that there is a population-level control exclusively during differentiation as growth during pluripotency is unaffected by the seeded number of cells. Furthermore, a differentiating ESC system exhibits a tipping point and show hints of critical slowing down. The petri dish size seems to be the scale at which the ESCs population collectively behaves during differentiation.

3.1.2 Differentiation Dynamics

Aside from growth dynamics, we were also interested in how successfully the ESCs can differentiate when varying the seeded number of cells. The 46C cell line has a GFP tag that is expressed when Sox1 is expressed. By using this cell line and measuring the GFP, the % of Sox1:GFP positive cells in a population could be measured. The % of Sox1:GFP positive cells in a population indicates the % of the population that has differentiated towards the NE lineage. Complementary to figure 3.3 (B), figure 3.8 shows the % of cells that are Sox1:GFP positive in a population for various cell seeding numbers. These are the same cells as in figure 3.3 (B), *i.e.* 46C cells were grown in N2B27 and refreshed with N2B27 + RA on day two. Not surprisingly, we find that there is a differentiation efficiency smaller than 100%, the highest observed % of Sox1:GFP positive cells is 73.44% $\pm$ 3.73 at $N_{seeded} = 175k$. When comparing the % of differentiated cells for a high seeded cells number $N_{seeded} = 300k$ with a % Sox1:GFP = 70.4% $\pm$ 2.73 to the % of differentiated cells for a low seeded cell number $N_{seeded} = 50k$ with % Sox1:GFP = 24.1% $\pm$ 8.49, we observe more than a two-fold difference. It also seems that the highest seeded density population ($N_{seeded} = 700k$) is not necessarily the population with the highest % of differentiated cells (% Sox1:GFP = 61.2% $\pm$ 2.18). These experiments show that aside from growth, the seeded number of cells also control the differentiation efficiency.

Therefore we combined to two datasets the 46C cell line into a three dimensional plot (time, N_{final}/N_{seeded} and N_{seeded}) with a colourmap that indicates the percentage of Sox1:GFP positive cells (figure 3.9). Two regions can be observed; the side of the low initial seeding densities is flat indicating that the cells barely grow in time. The cells plated at a higher initial seeding densities start expanding quickly after two to three days. The expansion overlaps with the largest percentage of Sox1:GFP positive cells, while the cells that did not grow well had the smallest percentage of Sox1:GFP positive cells. The highest seeding densities plateau and reach the carrying capacity after five days and have a lower percentage of Sox1:GFP positive cells than the cells that are actively still growing. These results show a correlation between population growth and differentiation.

In summary, these results show that aside from controlling growth, the seeded number of cells also control the differentiation efficiency of cells with a NE fate. Furthermore, results show a correlation between population growth and differentiation.

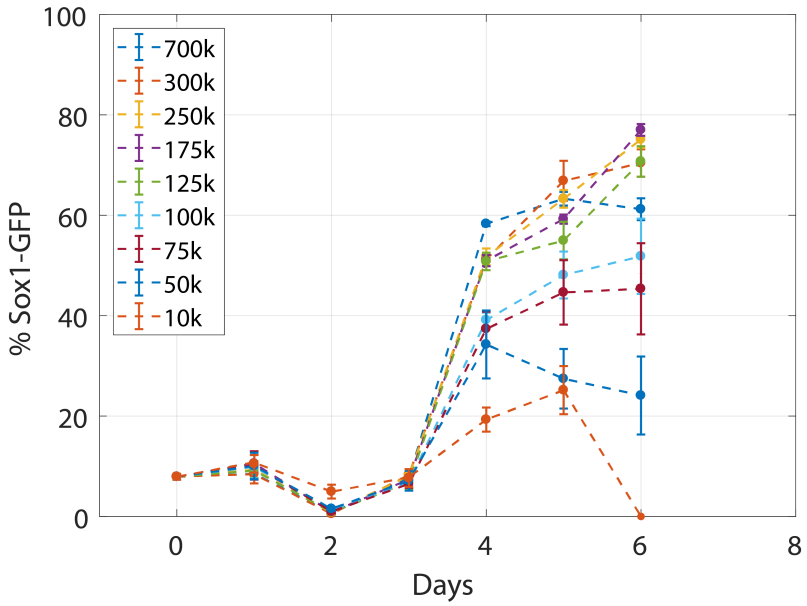

FIGURE 3.8: % of Sox1:GFP positive cells indicating the % of differentiated cells towards the NE lineage. 46C cells were grown on a $\varnothing 10cm$ dish in N2B27 medium which was refreshed with N2B27 + RA on day two. Different colours represent different seeded number of cells. % of Sox1:GFP positive cells in the population was measured using flow cytometry. Errorbars indicate the standard error of the mean of a minimum of three biological replicates.

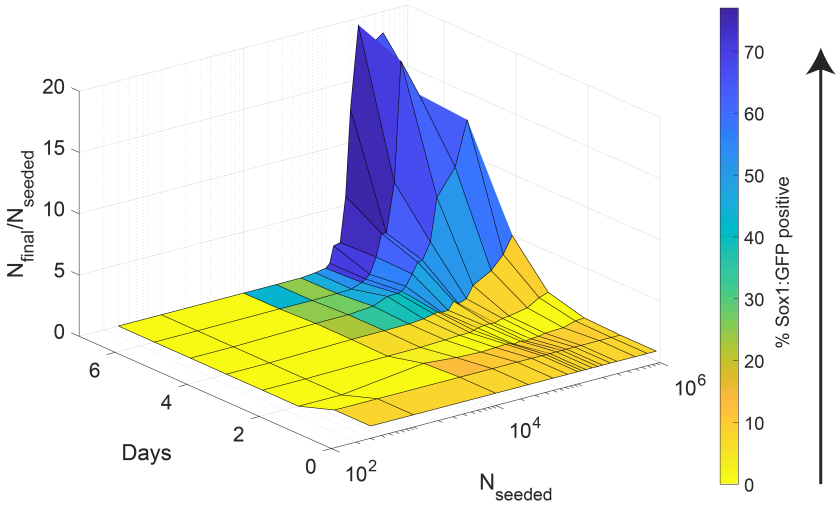

FIGURE 3.9: Growth differentiation landscape for NE differentiation. Colourmap represent the percentage of Sox1::GFP positive cells. 46C cells were grown on a $\varnothing 10cm$ dish in N2B27 medium which was refreshed with N2B27 + RA on day two. All data points are averages of at least three biological replicates. N_{final} was measured using a hemocytometer. % of Sox1:GFP measured using flow cytometry.

3.2 Colony-level

The next step aims at connecting the features from the population level with features from the colony level. We want to study how colonies exhibit the three previously found features (expansion, stationary, extinction). By using brightfield time-lapse microscopy we tracked colonies of E14 cells at high, medium and low seeding densities. For these experiments cells where grown on a $\varnothing 6cm$ dish instead of a $\varnothing 10cm$ dish. The cells were imaged in N2B27 for 96 hours, taking a snapshot every hour. In figure 3.10 a montage of ten frames of a 96 hour time-lapse of a high seeded density plate $N_{seeded} = 181k$ is shown. This timelapse shows that even for a high seeded density, cell death occurs at the first two days. The rest of the surviving colonies grow, merge and start changing their morphology as they differentiate. In contrast, almost all of the colonies at a low seeded density $N_{seeded} = 36k$ die in the first two days (figure 3.11).

Next we wondered if we could predict whether a cell or colony would die or survive based on simple properties of the colonies such as the area and the number of colonies in a field of view. By segmenting the cells in the timelapses, we were able to obtain the area and number of colonies in the field of view. Segmentation was done for high, medium and low seeded number of cells. Traces of the ratio of the area at time t and the initial area are shown in figure 3.12. The black lines represent the cells that are still alive after 96h, the green lines represent the cells that died and the red line is the mean of all the traces. Traces for the high number of seeded cells $N_{seeded} = 181k$ show that most of the colonies survive and grow exponentially in size. For the medium number of seeded cells $N_{seeded} = 90k$ most of the colonies died before the 96 hour mark. On average the colonies that do survive do not grow as well as the high initial density colonies. Traces of the low number of seeded cells $N_{seeded} = 36k$ show that there is close to no survival of colonies except for a spare few. In table 3.1 Fold increase of the mean area and the % of dead colonies after 97h are shown. As the seeded number of cells decreases the fold-increase in area decreases and the % of dead colonies increases. Similarly to the macroscopic population, these results show that whether a colony expands or goes extinct depends on the seeded number of cells. However, from these results we cannot predict whether a cell or colony would die based on the initial area.

We want to develop a model that provides the probability of survival for any initial colony area. The data of the initial areas can be plotted as a scatterplot with alive (1) or dead (0) on the y-axis and the initial areas on the x-axis. To model the probabilities of the cell surviving for each initial area we use logistic regression. Logistic regression can model the probability of an event (alive or dead) depending on values of independent variable(s) (initial colony area). The logistic regression model can predict the effects of a series of variables on a binary response variable. Binary data does not have a normal distribution, which is a condition for most other types of regressions, hence logistic regression is used. The goal of logistic regression is to estimate p for a linear combination of the independent variables.

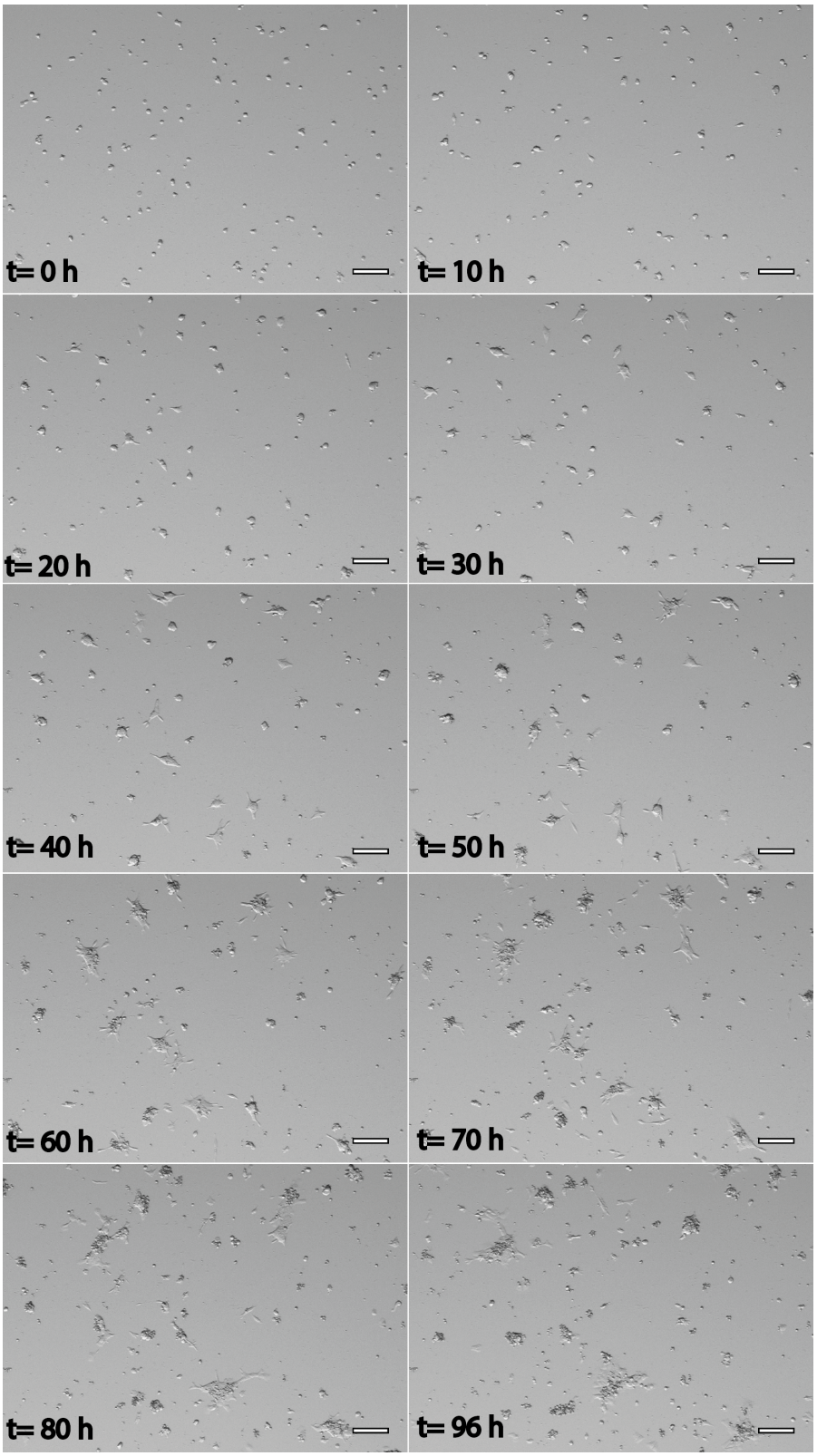

FIGURE 3.10: Frames of a microscopy timelapse of E14 cells grown in N2B27 at a seeding number of $N_{seeded} = 181k$ (k=1000) on a $\varnothing 6cm$ dish. Frames are shown with a 10 hour interval. Cell death occurs at the first two days. The rest of the surviving colonies expand and merge to form bigger colonies. Scale bar = $116\mu m$

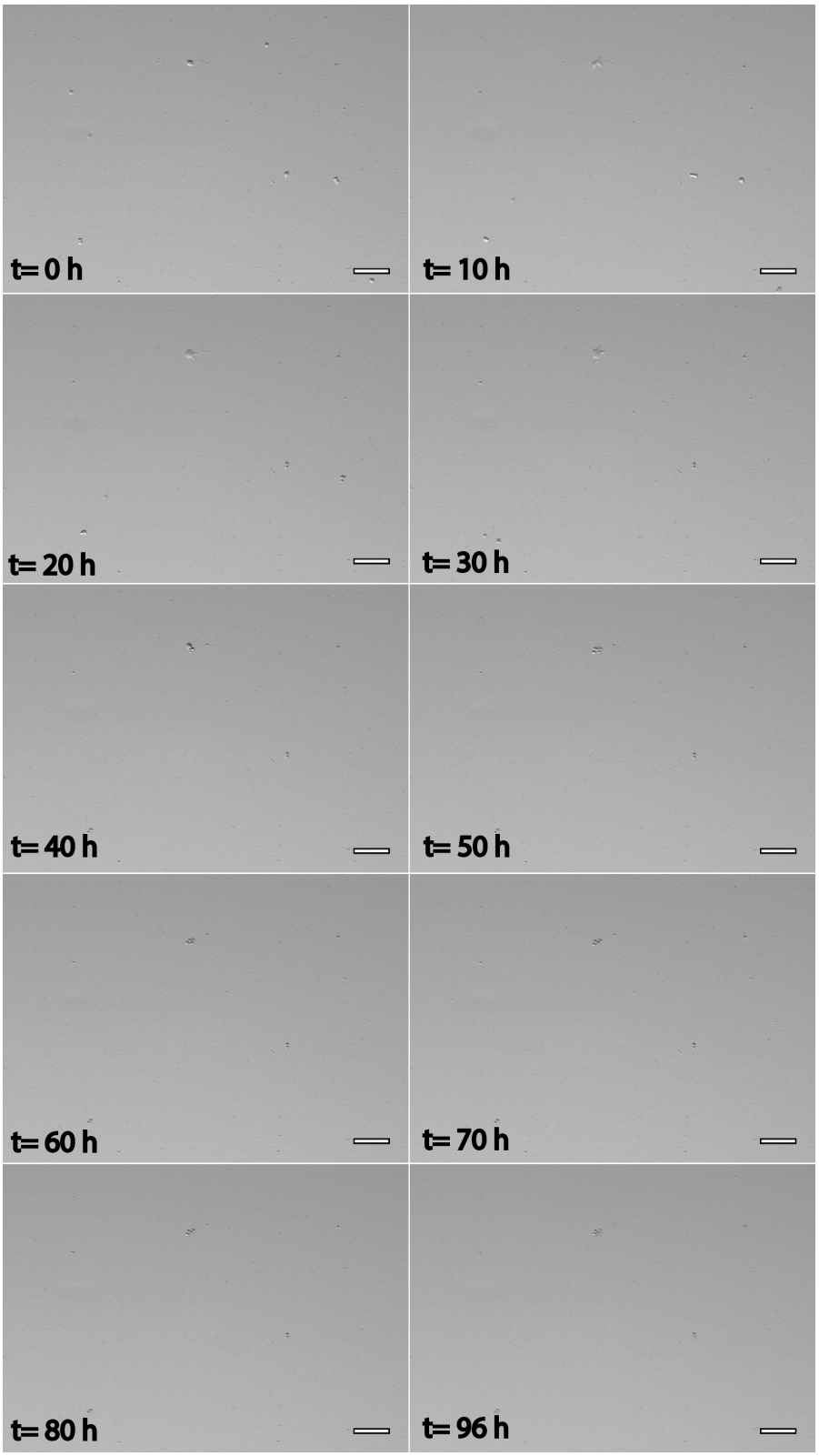

FIGURE 3.11: Frames of a microscopy timelapse of E14 cells grown in N2B27 at a seeding number of $N_{seeded} = 36k$ (k=1000) on a $\varnothing 6cm$ dish. Frames are shown with a 10 hour interval. All colonies die over the course of the time-lapse.

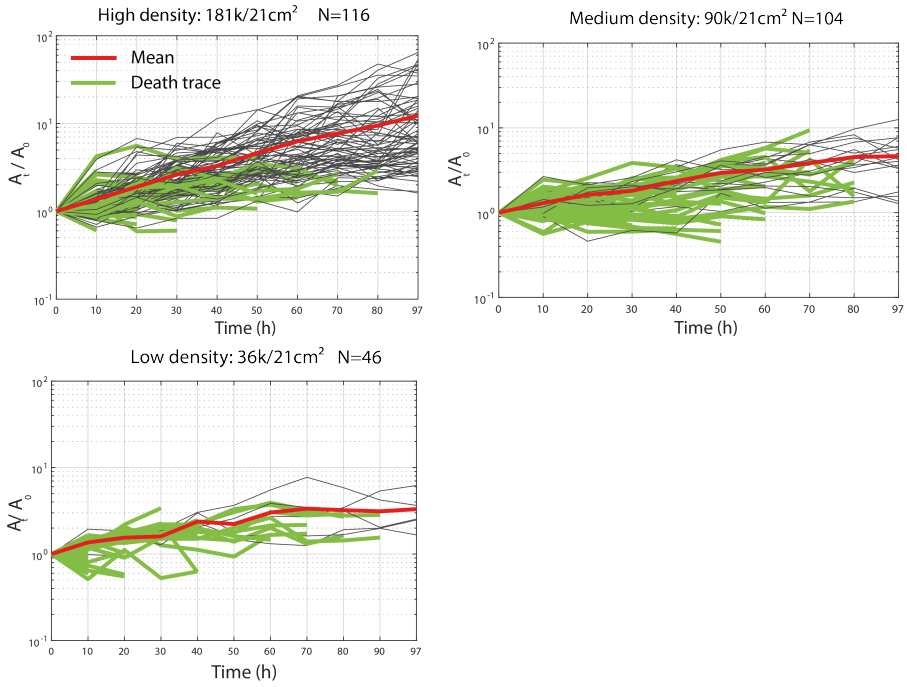

FIGURE 3.12: Area traces of 96 hours timelapses of high (181k), medium(90k) and low(36.2k) seeded densities (from left to right). E14 cells grown in N2B27 at a on a $\varnothing 6cm$ dish. Black lines indicate survival traces, green lines indicate traces that died and the red trace indicates the mean. The y-axis represents the ratio of area at time t and the initial area $\frac{A_t}{A_0}$.

	181k/$21cm^2$	**90k/**$21cm^2$	**36k/**$21cm^2$
Fold increase of area in 96 hours	≈ 10	≈ 5	≈ 2
% dead colonies after 96h	26.7	84.6	89.1

TABLE 3.1: Table showing the fold increase of the mean area traces in 96 hours (A_{96}/A_0) and % of dead colonies after 96h for $N_{seeded} = 181k$,$N_{seeded} = 90k$ and $N_{seeded} = 36k$ ($N_{deathcolonies}/N_{totalcolonies}$).

The logistic function is the inverse of the logit function:

$$logit(p) = ln(\frac{p}{1-p}) \leftrightarrow logit^{-1}(\alpha) = \frac{1}{1+e^{-\alpha}} = \frac{e^{\alpha}}{1+e^{\alpha}}$$

With α some number. The logit function is equivalent to a linear function of the independent variables.

$$logit(p) = ln(\frac{p}{1-p}) = \beta_0 + \beta_1 x_1$$

To find the estimated regression equation we need to solve above equation for p.

$$\frac{p}{1-p} = e^{\beta_0+\beta_1 x_1}$$

$$p = e^{\beta_0+\beta_1 x_1} - e^{\beta_0+\beta_1 x_1} \cdot p$$

$$p(1+e^{\beta_0+\beta_1 x_1}) = e^{\beta_0+\beta_1 x_1}$$

$$\hat{p} = \frac{e^{\beta_0+\beta_1 x_1}}{1 + e^{\beta_0+\beta_1 x_1}}$$

The coefficients β_0 and β_1 were estimated by using the mnrfit function in MATLAB. The function solves the estimations of the coefficients by using the maximum likelihood estimation (MLE). The independent variable x_1 represents the initial area. By using the estimated coefficients, estimated probability of dying given the initial area for the three initial densities can be plotted (3.13).

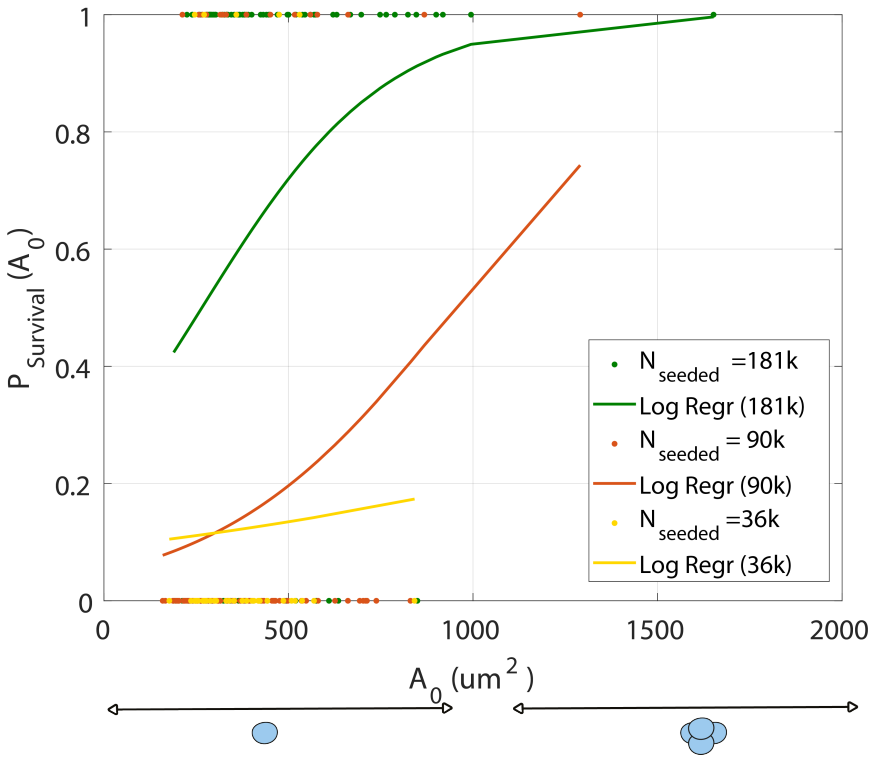

FIGURE 3.13: Summary plot of probability of surviving given the initial area $P_{Survival)(A_0)}$ determined by logistic regressions for three different conditions, $N_{seeded} = 181k$ (green), $N_{seeded} = 90k$ (red) and $N_{seeded} = 36k$ (yellow), $k = 1000$. Dots indicate whether a colony died (0) or survived (1) over the course of 96 hours. Probabilities are based on time-lapses in which E14 cells are grown on a $\varnothing 6cm$ dish in N2B27 for 96 hours.

In figure 3.13 the estimated probabilities of survival given the initial area are shown for the three seeded cell numbers. The low initial colony area are mostly single cells, while higher initial areas represent colonies that consists of multiple cells. It can be seen that for the high and medium seeded number of cell the probability of survival increases as the the initial area increases. The probability of survival for the low number of seeded cells seems to stay roughly constant independent of the initial area. These results indicate that the initial area of a colony is important for the survival at the higher range of seeded cell numbers. These results also show that the probability of survival for each initial area increases as the seeded number of cells increases. The probability of cell survival depends on the initial area and the seeded number of cells.

The second parameter we measured during the analysis is the number of colonies in the field of view. If the survival of colonies depends on the number of colonies in a field of view, then the collective behaviour of differentiating ESCs populations would matter on a local scale. In figure 3.14, estimated probabilites of survival given the initial area are shown for four fields of views plated at $N_{seeded} = 90k$. The figure shows that there is no increase in the probability of survival as the number of colonies in a field of view increases. These primary results hint that the local behaviour of colonies at the scale of the field of view is not important for the survival of colonies. However, from figure 3.13 we know that an increase in the number of seeded cells increases the probability of survival of the colonies. These results show that the scale at which the differentiating ESCs population collectively behave is larger than the field of view, confirming the results found at the population-level.

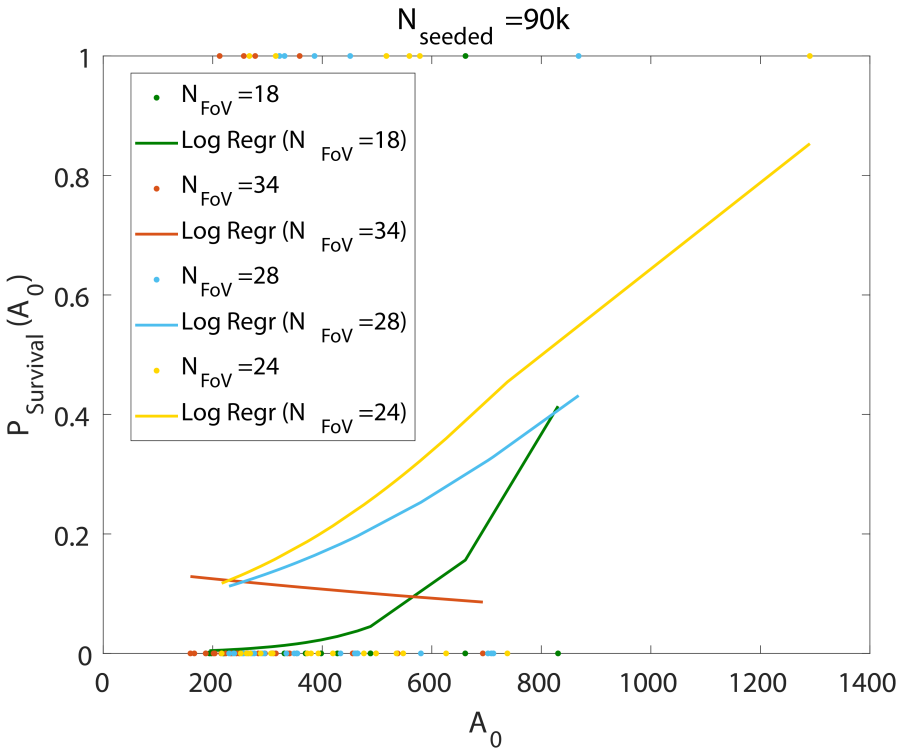

FIGURE 3.14: Summary plot of probability of surviving given the initial area $P_{Survival)(A_0)}$ determined by logistic regressions for four different conditions, $N_{FoV} = 18$ (green), $N_{FoV} = 34k$ (orange), $N_{FoV} = 28$ (blue) and $N_{FoV} = 24$ (yellow) at a seeding number of $N_{seeded} = 90k$, $k = 1000$. Dots indicate whether a colony died (0) or survived (1) over the course of 96 hours. Probabilities are based on time-lapses in which E14 cells are grown on a $\varnothing 6cm$ dish in N2B27 for 96 hours.

In summary, we found two density-dependent features at the colony level that are also present at the population-level, *i.e.* expansion and extinction. The stationary phase remains to be found. The result show that the probability of survival of colonies depends on the seeded density and the initial area of the colonies. However, the probability of survival seems to be independent of the number of colonies in the field of view, suggesting that the scale of collectivity of differentiating ESCs is larger than the field of view.

3.3 The Search for a Molecular Mechanism

Next we turned to the molecular mechanism underlying the density dependent population behaviour of differentiating ESCs. Cells communicate by signalling molecules. One possibility is that adjacent cells transmit signals to each other such that cells need to be in contact to communicate, this form of cellular communication is known as juxtacrine signalling. Another option is the secretion of a soluble factor in the medium that diffuses towards neighbouring cells. We wondered what happens if we take the environment (*i.e.* culture medium) of cells seeded at a high density (population expands) to cells seeded at a low density (population goes extinct). We designed an experiment in which we transfer the medium of cells that are plated on a $\varnothing 10cm$ dish at a high seeded density ($N_{seeded} = 300k$) to low seeded density ($N_{seeded} = 50k$) (figure 3.15). For this experiment 46C cells were used. The cells from which the medium is transferred are grown in N2B27 and refreshed with N2B27+RA on day two. This experiment was done over a period of six days. Some controls were performed to make sure that the observed effects were a consequence of the transferring of the medium. One control showed that no cells are brought over during the medium transfer process.

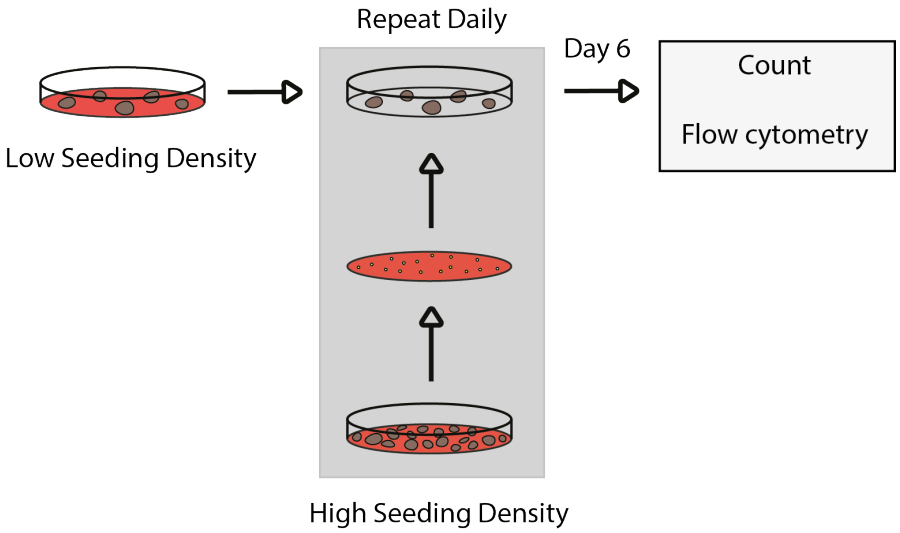

FIGURE 3.15: Schematic overview of the medium transfer experiment. High seeding density cells are grown on a $\varnothing 10cm$ dish in N2B27 and refreshed with N2B27+RA on day two. Medium is transferred daily from initially high seeded density cells to low seeded density cells for a period of six days. At the sixth day the cells are counted using a hemocytometer and fluorescence is measured using flow cytometry.

Figure 3.16 shows that transferring the medium every day for a period of six days enabled the low seeded density population to expand instead of going extinct. A control was done to make sure that the observed result is not a consequence of giving the cells new nutrients daily. The microscopy images (figure 3.17) of the transfer experiment show that there are more cells and that the morphology of the cells has changed over the course of six day. Furthermore, the percentage of differentiated cells also increased significantly. The results of this experiment leaves out a molecular mechanism in which juxtracrine signalling is important, since only the culture medium is transferred.

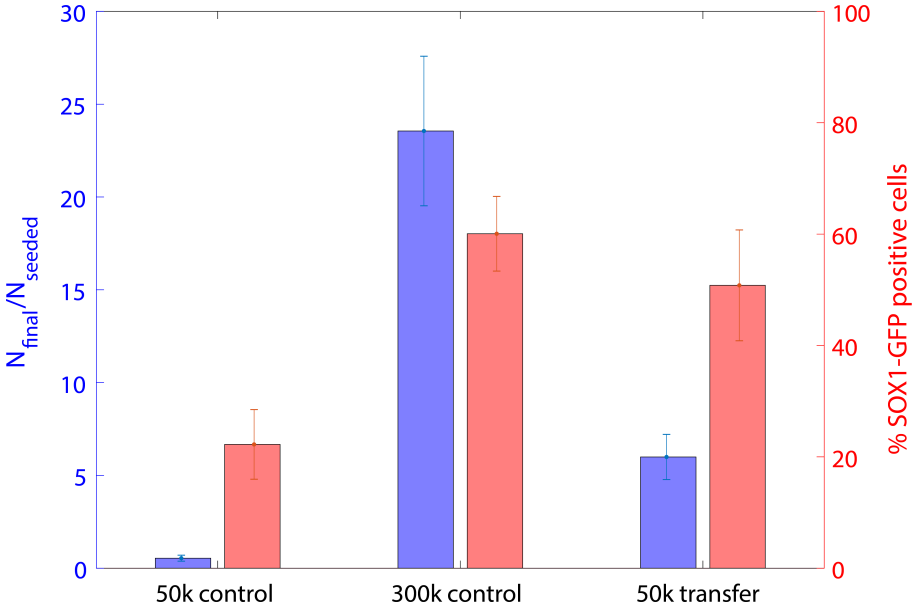

FIGURE 3.16: Bar plot showing N_{final}/N_{seeded} (blue) and $\%Sox1 : GFPpositivecells$ (red) of 46C cells at $N_s = 50k$ (left), $N_s = 300k$ (middle) and $N_s = 50$ with daily medium transfer (right). N_{final} was measured with a hemocytometer. The $\%Sox1 : GFPpositivecells$ was measured using flow cytometry. The controls were grown on a $\varnothing 10cm$ dish in N2B27 and refreshed with N2B27 + RA on day two. The error bar indicates the standard error of the mean of a minimum of three biological replicates.

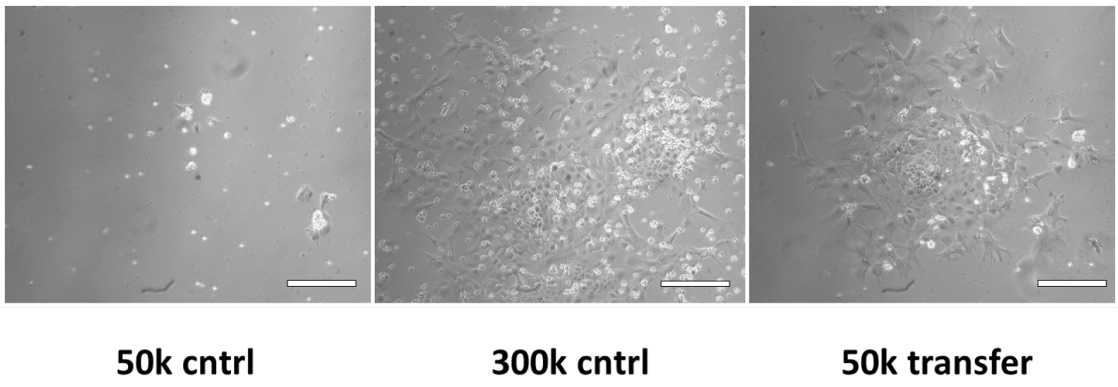

FIGURE 3.17: Microscopy snapshots of 46C cells at $N_s = 50k$ (left), $N_s = 300k$ (middle) and $N_s = 50$ with daily medium transfer (right). The controls were grown on a $\varnothing 10cm$ dish in N2B27 and refreshed with N2B27 + RA on day two. Scale bar = $200\mu m$.

Probably, a soluble factor secreted by the cells seeded at a high density is responsible for the survival of the cells seeded at a low density. In a follow up experiment, we refreshed the medium of different initial density with fresh medium daily (figure 3.18. The cells that were refreshed daily showed less growth and a smaller % of the population was Sox1 positive. However, it is not clear whether the observed result is a consequence of the daily addition of fresh (toxic) RA or something else.

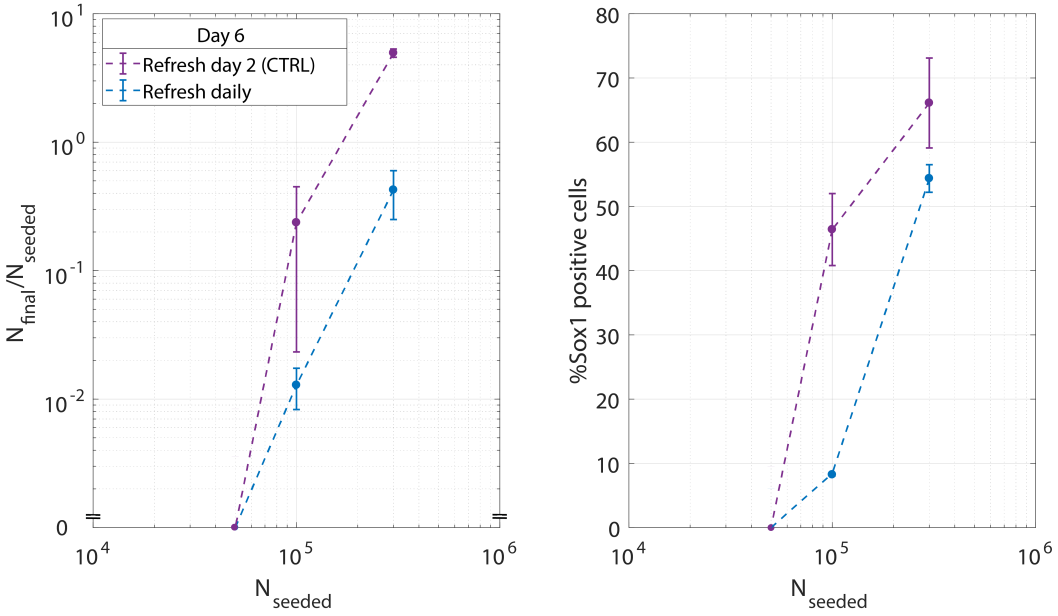

FIGURE 3.18: Graph showing N_{final} / N_{seeded} and the % of Sox1 positive cells in a condition in which the medium of 46C cells grown on a $\varnothing 10cm$ dish was refreshed daily (blue) and a control in which the medium was refreshed solely on the second day (purple). The medium was refreshed with N2B27 + RA.

To find possible candidate molecules for a suitable biological mechanism, Hirad Daneshpour performed RNA-sequencing on a number of different samples with different initial cell densities on different days. The conditions consist of a pluripotent control (CD0F), $N_{seeded} = 800k$ grown for two days in N2B27 (S800kD2N) and $N_{seeded} = 800k$ (S800kD4NR), $N_{seeded} = 200k$ (S200kD4NR), $N_{seeded} = 100k$ (S100kD4NR) grown for four days in N2B27, refreshing the media on day two with N2B27+RA. All RNA sequencing was performed on RNA of the wild type (E14) cell line. A heatmap with a list pluripotent gene expression for the different conditions is shown in figure 3.19. The heatmap shows, as expected, that the pluripotent genes are more highly expressed in the control sample when compared to the other samples. This is a good indication that the RNA-sequencing and analysis worked properly, a similar heatmap was made for genes that are expressed in cells that differentiated to the NE-lineage (figure appendix B.5).

On figures 3.20 and 3.21 , heatmaps of important pro- and anti apoptotic factors can be found. Apoptotic and anti apoptotic factors play a crucial role in the surival of a cell. The balance of the activity of anti- and pro apoptotic factors can determine whether a cell will go into apoptosis or not. Upon withdrawal of the pluripotent state, overexpression of an antiapoptotic factor Bcl2 can prevent apoptosis [75]. Differentiation and apoptosis have been linked before *in vivo* [76]. The first days after leaving the pluripotent state are crucial for the cells. The expression of the pro apoptotic genes seems to be rather constitutively, however, the expression of anti apoptotic genes seems to turn on after cells leave their pluripotent state. Interestingly as in Duval *et al.*, Bcl2 starts to be expressed after withdrawal of the pluripotent state [75]. Furthermore, it seems that the expression of Bcl2 is highest for the highest seeded density (S800kD4NR).

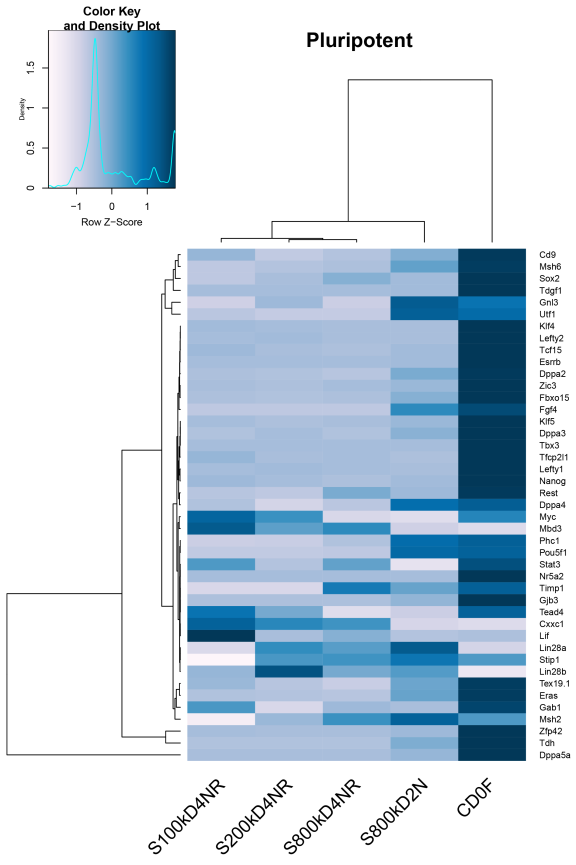

FIGURE 3.19: Heatmap showing expression of pluripotent genes for the five different conditions. The conditions consist of a pluripotent control (CD0F), $N_{seeded} = 800k$ grown for two days in N2B27 (S800kD2N) and $N_{seeded} = 800k$ (S800kD4NR), $N_{seeded} = 200k$ (S200kD4NR), $N_{seeded} = 100k$ (S100kD4NR) grown for four days in N2B27, refreshing the media on day two with N2B27+RA. Light blue represents low expression and dark blue represents high expression.

This density dependent expression might indicate that expression of Bcl2 plays a part in the molecular mechanism that behind density depended population behaviour. However, Bcl2 is not a signalling molecule. *Duvel et al.* describe the expression of Bcl2 as an reaction to the removal of the signalling molecule LIF [75]. RNA-sequencing also showed that LIF is slightly expressed in the differentiating samples (figure 3.18).

Expression of LIF might hint to a mechanism in which LIF is signalled between the neighbouring cells to promote survival. To further investigate the molecular mechanism we performed RT-qPCR on low and high seeded cell densities ($N_{seeded} = 50k$ and $N_{seeded} = 300k$) at day one and day two in N2B27 medium. RT-qPCR was performed on a set of genes active in apoptosis and the LIF gene (figure 3.22). The results suggest that the high seeded density has a higher expression of the anti apoptotic genes when compared to the low seeded density. The apoptotic genes seem to be constitutively expressed for both cases, indicating that the increase in expression of the anti apoptotic genes might determine the survival of a population. LIF also has a higher expression in the high seeded density condition when compared to the low seeded density condition.

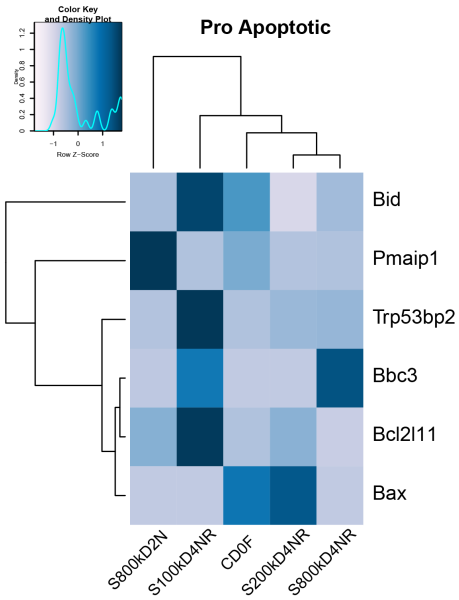

FIGURE 3.20: Heatmap showing expression of pro apoptotic genes for the five different conditions. The conditions consist of a pluripotent control (CD0F), $N_{seeded} = 800k$ grown for two days in N2B27 (S800kD2N) and $N_{seeded} = 800k$ (S800kD4NR), $N_{seeded} = 200k$ (S200kD4NR), $N_{seeded} = 100k$ (S100kD4NR) grown for four days in N2B27, refreshing the media on day two with N2B27+RA. Light blue represents low expression and dark blue represents high expression.

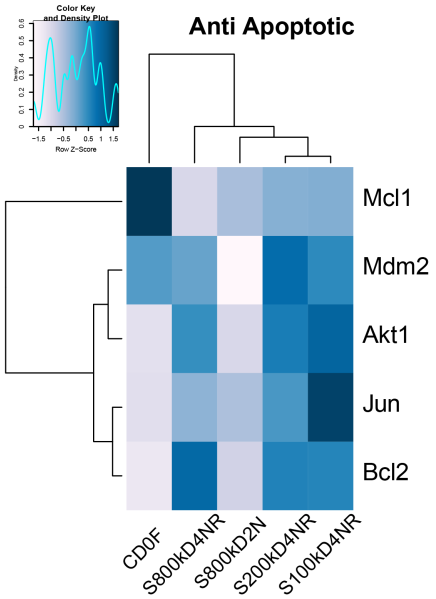

FIGURE 3.21: Heatmap showing expression of anti apoptotic genes for the five different conditions. The conditions consist of a pluripotent control (CD0F), $N_{seeded} = 800k$ grown for two days in N2B27 (S800kD2N) and $N_{seeded} = 800k$ (S800kD4NR), $N_{seeded} = 200k$ (S200kD4NR), $N_{seeded} = 100k$ (S100kD4NR) grown for four days in N2B27, refreshing the media on day two with N2B27+RA. Light blue represents low expression and dark blue represents high expression.

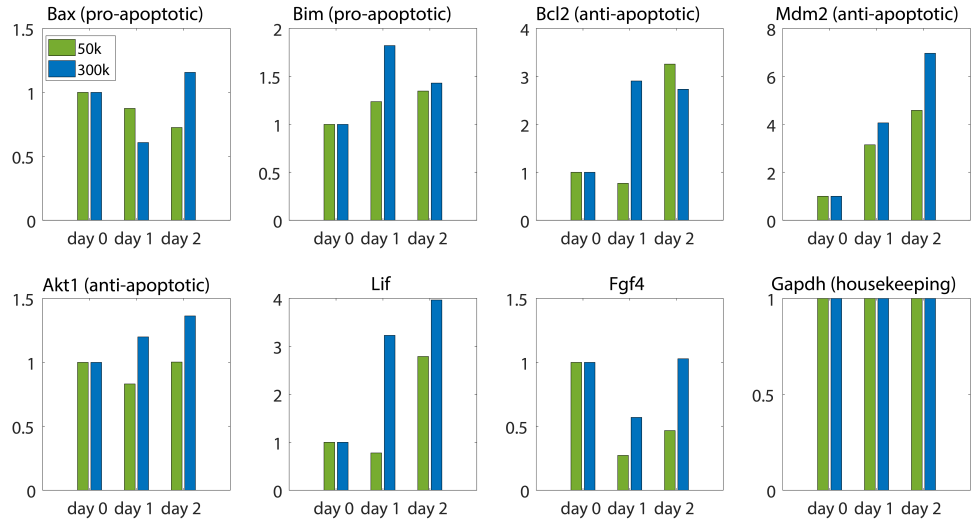

FIGURE 3.22: RT-qPCR performed on RNA from the wildtype (E14) cell line at $N_s = 50k$ (green) and $N_s = 300k$ (blue) grown in N2B27 for one or two days. Expression was normalized using a housekeeping gene GAPDH. The fold enrichment was calculated by using the $2^{\Delta\Delta C_t}$ method [67]. Data from one biological replicate

Aside from these results, we also wondered whether cells at a low seeded density are pluripotent for a longer time than the cells at a high seeded density. For these experiments, the cell lines with the GFP-tagged pluripotency markers were used. The markers Nanog (E14/N14) and Oct4 (O4G) are active when cells are in a pluripotent state. Cells were set up at different seeded densities over a period of hours (E14/N14 cell line) or days (O4G cell line) in N2B27, refreshing with N2B27 + RA on day 2. The % of Nanog (fig. 3.23) or Oct4 (fig. 3.24) positive cells was measured using flow cytometry.

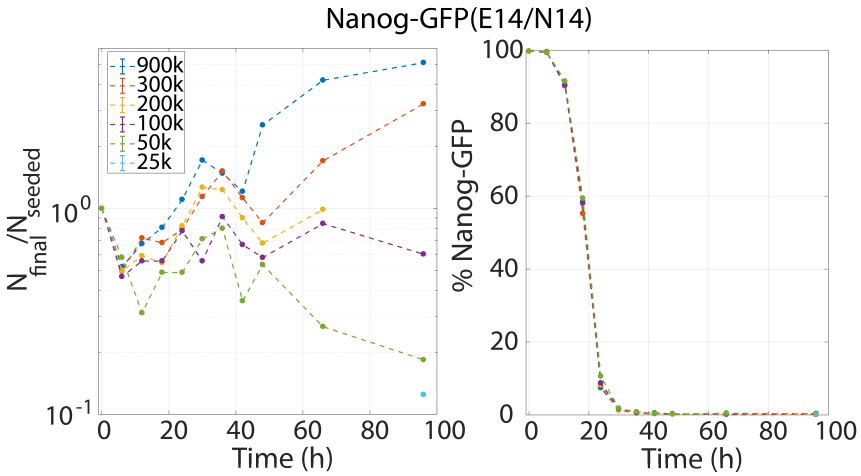

FIGURE 3.23: Growth (left) and differentiation (right) dynamics of the Nanog-GFP (E14/N14) cell lines at various seeding densities (different colours). Cells were on a $\varnothing 10cm$grown in N2B27 and refreshed with N2B27+RA on day two. N_{final} was measured using a hemocytometer. % Nanog-GFP was measured using flow cytometry. Data based on a single biological replicate.

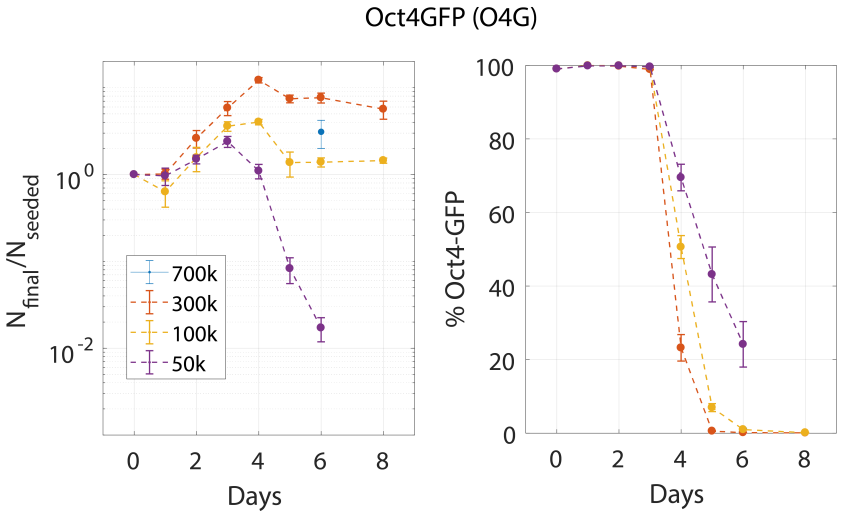

FIGURE 3.24: Growth (left) and differentiation (right) dynamics of the Oct4-GFP (E14/N14) cell lines at various seeding densities (different colours). Cells were on a $\varnothing 10cm$grown in N2B27 and refreshed with N2B27+RA on day two. N_{final} was measured using a hemocytometer. % Oct4-GFP was measured using flow cytometry. Error bars indicate standard error of the mean of a minimum of three biological replicates.

Figure 3.23 shows that the drop of % of Nanog positive cells is not dependent on the seeding density. However, figure 3.24 show that the drop of % of Oct4 positive cells depends on the seeded density. The higher the seeded density the faster the amount of Oct4 positive cells drops (*e.g.* compare the % of Oct4GFP at day 5 for $N_{seeded} = 50k$ and $N_{seeded} = 300k$. These results indicate that populations at a low seeded density take longer to turn off Oct4 expression, in other words a fraction of the population remains pluripotent.

In summary, the biological mechanism behind the density dependent population behaviour mainly depends on a soluble factor secreted into the medium. Furthermore, the regulation of expression of anti and pro apoptotic factors could determine whether a population survives or not. A mechanism involving LIF is plausible, as the qPCR shows that LIF is expressed at a high level in cells seeded at a high density.

3.4 A Model for Collective Survival

The main focus of this thesis is on the biological experiments, however, we wondered if a model could answer whether the secretion of one type of signalling molecule is a possible explanation for the three observed features (expansion, stationary and extinction) in populations of differentiating ESCs. In this primary model the secretion of a molecule by a cell is modelled mathematically by the reaction-diffusion equation. The reaction-diffusion equation that models the concentration of a molecule in space and time.

$$\frac{\partial M}{\partial t} = D_M \nabla^2 M + R(M)$$

By using the approach as in Olimpio *et al.*, we obtain the steady state solution for the concentration of M [77].

$$M(r) = \frac{c_R R}{r} e^{(r-R)/\lambda}$$

with

$$c_R = \frac{\eta\gamma}{4\pi R\lambda(\lambda + R)}$$

$\lambda = \sqrt{\frac{D_M}{\gamma}}$ is the diffusion length, η the secretion rate of the cells, γ the degradation rate of the molecule and R the radius of the cell.

The model starts with the (uniformly) random placement of cells on a circle. A circle was chosen because cells are grown in circular plates during experiments. These cells have 3 potential actions that are governed by a simple set of rules; the cells can die, divide or remain senescent. Each cell is a source of the signalling molecule M. The concentration of M is determined by the reaction-diffusion equation shown above. Each x timesteps cells will decide whether they are going to divide or remain senescent. The choice depends on the concentration of signalling molecule present at the location of the cell. If the local concentration of signalling molecules is higher than a certain threshold, cells will choose to divide. Otherwise cells will be in a senescent state and essentially do nothing. During division the daughter cell will locate on one of the 8 pixels that is surrounded by the mother cell, if all 8 neighbouring pixels of the mother cell are already occupied by other cells, the mother cell will automatically go into a senescent state. Cells die if they have been in a senescent state for three events in a row. A schematic overview is shown in 3.25.

The model was run for a set of seeded number of cells. When finished, the growth was measured. The simulation was run for 400 timepoints. The parameters used for the reaction-diffusion equation listed in the appendix. Figure 3.26 shows N_{final}/N_{seeded} after 400 points for the set of seeded number of cells. The result is similar to the experimental result, *i.e.* populations at high N_{seeded} survive and populations at low N_{seeded} show an extinction trend. These result show that in our specific model the secretion and sensing of a single signalling molecule enables the population to collectively survive or collectively go extinct. To find out whether a stationary population is also present in the model, we plotted the growth in time of the N_{seeded} at which N_{final}/N_{seeded} is approximately one (figure 3.27). Figure 3.27 shows there is no such stationary population. The population of $N_{seeded} = 2481$ first dips and then expands. However, we have not tried changing the parameter values which might enable a stationary population to occur in the model.

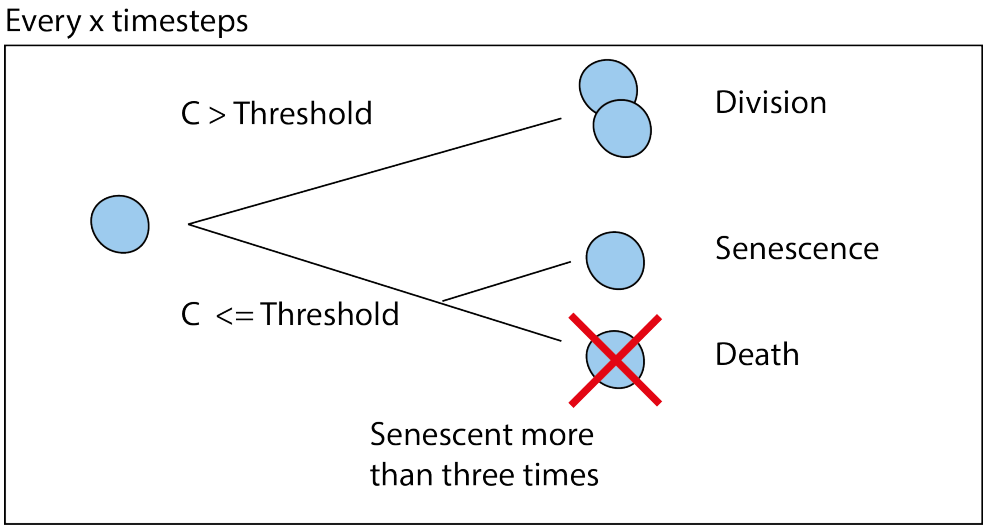

FIGURE 3.25: Schematic overview of the possible actions of a cell in the model. Every x timesteps the cell measures the concentration of the signalling molecule (C). When higher than a certain threshold the cell will divide. If the concentration is lower the cell will remain senescent. If the cell is senescent for three actions in a row the cell will die.

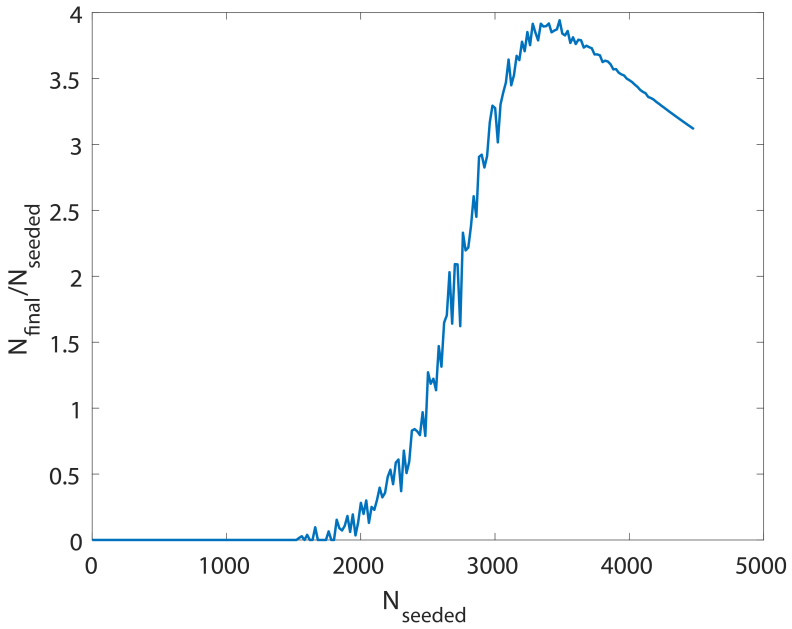

FIGURE 3.26: Plot of growth ($\frac{N_{final}}{N_{seeded}}$) versus the seeded number of cells N_{seeded}. Cells were uniform randomly distributed on a circle with a radius of 66 pixels and simulated for 400 timesteps. Every 40 timesteps cells would undertake one action(divisions, senescence or dead). Plot is the average of three simulations.

In summary, for this particular model the secretion and sensing of a single signalling molecule enables density dependent population survival behaviour. However, no stationary population was found.

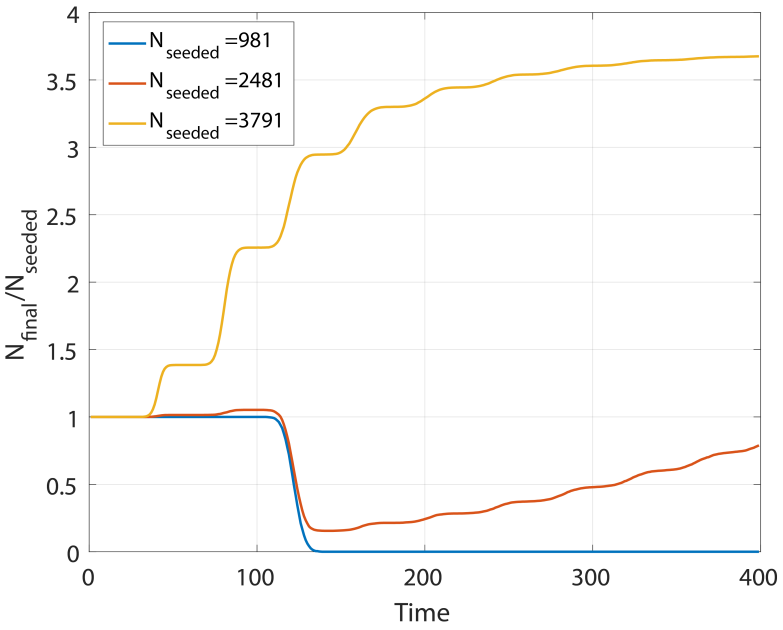

FIGURE 3.27: Growth dynamics of a set of three seeded number of cells. Cells were uniform randomly distributed on a circle with a radius of 66 pixels and simulated for 400 timesteps. Every 40 timesteps cells would undertake one action(divisions, senescence or dead). The waviness of the plot is due to that all cells are synchronized. Plot is the average of three simulations.

Chapter 4

Discussion

So far results have shown that there are signs of macroscopic collective behaviour in differentiating ESC populations. However, experiments still have to be done to verify critical slowing down in the differentiating stem cell system. Critical slowing down can be verified by studying the variation in population number of different biological replicates of cells growing in differentiation medium for 15 days. An increase in variation should be observed when plating a large number of biological replicates at different N_{seeded} close to the the critical threshold. In addition a control with the N_{seeded} that reaches the carrying capacity and the N_{seeded} which goes extinct should be done. These controls should have a low variation in population number since all biological plates should either reach the carrying capacity or go extinct.

The three main features of the population are survival, dead and a stationary population and depend on the seeding density of the cells. Is there a biological reason that populations can express these three features? For a pregnant mother mouse, it might be beneficial for the embryo to self-destruct when there are too few cells to develop into a functional embryo, especially when resources are limited. The stationary population of the cells could resemble the *in vivo* embryonic diapause in mice, a mechanism in which the embryo remains delayed in the blastocyst stage. The main function of the embryonic diapause is to control when the birth takes place, to avoid unfavourable conditions at the time of birth. *In vivo* experiments have shown that blastocyst may enter the diapause state in the absense of LIF [78]. Furthermore, researchers have shown that blastocyst with a knock out of the Gp130 gene, a component of the LIF receptor, gradually lose their ICM cells and lose their ability to survive [79]. These *in vivo* studies hint at the important role of LIF (or another factor that binds to Gp130) in regulating blastocyst survival and embryonic diapause. The importance of LIF and/or Gp130 in the survival of *in vitro* populations remains to be tested. Since cells in the embryonic diapause also remain in a pluripotent state, the embryonic diapause could also be an explanation for the results that show that it takes longer to turn of Oct4 expression for the cells that show an extinction growth profile. The diapause would link both observed results. A time-lapse microscopy experiment in which the GFP of O4G cells is imaged for a period of 96 hours in differentiation medium can show whether it are the pluripotent cells that are unable to differentiate that die or not.

Although experiments have shown hints for a possible molecular mechanism, follow-up experiments are necessary. The autosecretion of LIF might be a plausible candidate. So far, the experiments only consisted of studying the transcript level of LIF in the cell. To verify LIF as candidate, RT-qPCR for LIF should be performed on more conditions, *i.e.* three and four days after differentiation at a high and low

initial density. We need to be careful when taking the RNA-seq and RT-qPCR data into account, since these experiments only show what happens on a transcript level and not on a protein level. Proteins of a gene do not have to be active even though transcription of the gene is elevated. Proteins can be activated or inactivated by *e.g.* phosphorylation by protein kinases. To verify a molecular mechanism experiments which alter the gene at a protein level are necessary. For this reason an experiment in which LIF expression is knocked out in cells that are plated at a high initial density would complement the data.

Aside from LIF there might be other possible candidates. One is the auto-secretion of Fgf4. Fgf4 is a protein that is important for both survival and differentiation. Fgf stimulation of the MAPK pathway is necessary for ESCs to commit to a lineage [52]. Another interesting candidate is Cyclophilin A which increases the growth rate of mouse ESCs in dose-dependent manner [80]. The last candidate is the stromal cell-derived factor (SDF)-1/CXCL12 which is secreted by mESCs and increases survival and differentiation [81].

The experiments in which the medium of cells was refreshed daily with N2B27+RA showed that cells were able to grow less and that a smaller % of the population was able to differentiate. One reason might be that the addition of fresh RA is toxic to the cells, however another option is that cells need to be exposed to the signal for a certain amount of time. Aside from these results, we also have data in which we show that the timing of giving the differentiation signal CHIR matters. In these experiments cells of the Brachyury-GFP cell line were exposed to the signalling molecule CHIR at a certain day after plating for a certain amount of time (figure 4.1). On the fourth day the amount of Brachyury was measured with flow cytometry. As expected, cells that are exposed to CHIR for 48 hours, two days after plating, are Brachyury positive. Interestingly cells that are exposed to CHIR for 24 hours, two days after plating, are Brachyury postive as well. This result is in contrast to cells that are exposed to CHIR for 24h, three days after playing, which are Brachyury negative. Cells exposed to CHIR for less than 24h always ended up Brachyury-negative. These results suggest that mESCs have an open time window in which they are able to respond to a certain signal that can guide differentiation towards the ME or NE lineage. In a follow up experiment, we exposed cells to CHIR for 24h on the second day after which the cells were collected and seeded on a new plate. The amount of Brachyury postive cells was measured two days after replating. We wondered whether re-plating the cells would interfere with the communication network of the cells. The result was a decrease in differentiation efficiency, 29.2% of the population was Brachyury positive in comparison to the 78.7 % of the control population which was not re-plated. Diluting the population (1:5) during the re-plating process resulted in an even lower differentiation efficiency (22.5 % of the population was Brachyury positive). These experiments show that re-plating cells after being exposed to a signal has an effect on differentiation efficiency. It would be interesting to find out whether cells are able to remember whether they have seen the signal or not. An experiment in which cells are frozen after being exposed to a signalling molecule (RA or CHIR) for 24 hours could give insights in the potential memory of mESCs.

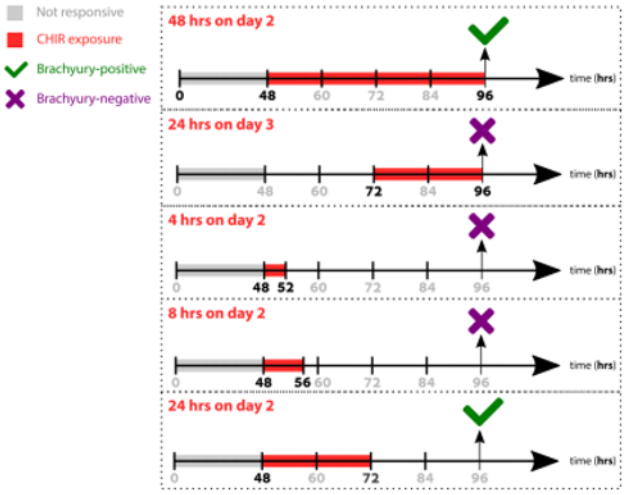

FIGURE 4.1: Figure illustrating the necessary exposure time and timing of the cells to CHIR (red) to successfully differentiate towards the mesendoderm lineage. Figure made by Hirad Daneshpour.

Analysis of the time-lapse microscopy showed that two features of the population-level also occur at a colony-level (expansion and extinction). However, the stationary population remains to be found. For time-lapse microscopy it is necessary to grow cell on $\varnothing 6cm$ plates instead of the for the main part used in this thesis $\varnothing 10cm$ plates. The conversion of the N_{seeded} at which a stationary population occurs on a $\varnothing 10cm$ plate to a $\varnothing 6cm$ plate is not as simple as multiplying the N_{seeded} with the ratio of the areas of the plates (see figure appendix B.4). However, it would be good to explore the features of a stationary population on a colony level to find out whether all colonies remain stationary or that the growth rate and the death rate of the population are equal.

The microscopy analysis also showed that probability of survival is independent of the number of colonies in a field of view the size of $1mm$ x $1.4mm$, suggesting that the scale of collectivity of differentiating mESCs is larger than the field of view. It is important to take into account that for these field of view logistic regressions only a small sample number was used so far. More data is required to completely verify these findings. Future experiments could focus on doing the same kind of analysis but with an increased size of the field of view. The results of these experiment could potentially quantify the scale at which differentiating ESCs behave collectively.

Although the main focus of this thesis was on the biological experiments and their results, we managed to build a simple preliminary model in which the secretion and sensing of a single signalling molecule allows for density dependent survival, but not for a stationary population. The model can be explored further by changing its parameter values to see if changing the parameter values enables a density dependent stationary population. The parameter values for the steady state reaction-diffusion equation were based on published biological parameters for proteins of the Interleukin (IL) family [82], since LIF is an IL-6 class cytokine. Instead of changing the parameter the model could also be changed to include a negative feedback system that inhibits secretion of the signalling molecules by cells when the local concentration of the signalling molecule is high. Although the model is interesting, it is not necessary to unravel the biological mechanism.

Appendix A

RT-qPCR

A.1 RT-qPCR amplification program

RT-qPCR Amplification program			
Step	**Temperature**	**Time**	**Cycle**
Polymerase activation and DNA denaturation	95°C	30s	1
Denaturation Annealing+Extension	95°C 60°C	15s 15s	35-40
Melt curve analysis	From 65°C to 95°C with 0.5°C increments	2-5s/increment	1

A.2 Primers for RT-qPCR

Primer name	Sequence	Description
mHP001	CGGAAGAGAAAGCGAACTAGC	Oct4 forward primer for RT-qPCR
mHP002	ATTGGCGATGTGAGTGATCTG	Oct4 reverse primer for RT-qPCR
mHP003	GCGGAGTGGAAACTTTTGTCC	Sox2 forward primer for RT-qPCR
mHP004	GGGAAGCGTGTACTTATCCTTCT	Sox2 reverse primer for RT-qPCR
mHP005	CACAGTTTGCCTAGTTCTGAGG	Nanog forward primer for RT-qPCR
mHP006	GCAAGAATAGTTCTCGGGATGAA	Nanog reverse primer for RT-qPCR
mHP007	AGAAGCCATAGTCGTGCCTGTGT	Gp130 forward primer for RT-qPCR
mHP008	AAAGCAGAACAAGACGCCCAGCA	Gp130 reverse primer for RT-qPCR
mHP009	CTTCGATCCTCAACCAGAGC	Lifr forward primer for RT-qPCR
mHP010	TGGTTAGTGCACCCATAGAGG	Lifr reverse primer for RT-qPCR
mHP011	GGATCGCTGAGGTACAACCC	Stat3 forward primer for RT-qPCR
mHP012	GTCAGGGGTCTCGACTGTCT	Stat3 reverse primer for RT-qPCR
mHP013	GGATACCAACTGTTACGTTCCATAATT	Lifrbeta forward primer for RT-qPCR
mHP014	TATCGAGTCTGCCGACGTATCTT	Lifrbeta reverse primer for RT-qPCR
mHP015	TGCAGCTCATGGGTCAAATC	Lif forward primer for RT-qPCR
mHP016	AACTGGCCCAGCTTTTTCTG	Lif reverse primer for RT-qPCR
mHP017	GTTTTTTGTAGTTGTTACCGC	Sox1 forward primer for RT-qPCR
mHP018	GCATTTACAAGAAATAATAC	Sox1 reverse primer for RT-qPCR
mHP019	CTGTGACTGCCTACCAGAATGAGGAG	Brachyury forward primer for RT-qPCR
mHP020	GGTCGTTTCTTTCTTTGGCATCAAG	Brachyury reverse primer for RT-qPCR
mHP021	GGGGCACGGCTGGGACG	Fgf4 forward primer for RT-qPCR
mHP022	CCCGTTCTTACTGAGGGCC	Fgf4 reverse primer for RT-qPCR
mHP023	GAAAAGACAGGCCGAGAGTG	Fgf5 forward primer for RT-qPCR
mHP024	GAAGTGGGTGGAGACGTGTT	Fgf5 reverse primer for RT-qPCR
mHP025	TGTAAGGACGAAACGGGACT	Mcl1 forward primer for RT-qPCR
mHP026	AAAGCCAGCAGCACATTTCT	Mcl1 reverse primer for RT-qPCR
mHP027	GGCTGCCAGGACGTCTCCTC	Bcl2 forward primer for RT-qPCR
mHP028	ATCCAGGTGTGCAGATGCC	Bcl2 reverse primer for RT-qPCR
mHP029	GAAGGAGGAAACGCAGGACA	Mdm2 forward primer for RT-qPCR
mHP030	CCTGGCAGATCACACATGGT	Mdm2 reverse primer for RT-qPCR
mHP031	AGCCTACCAACGTGAGTGCT	cJun forward primer for RT-qPCR
mHP032	AGAACGGTCCGTCACTTCAC	cJun reverse primer for RT-qPCR
mHP033	AGTGGACCACAGTCATTGAGC	Akt1 forward primer for RT-qPCR
mHP034	TTGAGTCCATCTGCCACAGTC	Akt1 reverse primer for RT-qPCR
mHP035	TATCGAAACCAGAGCGATGC	Trp53bp1 forward primer for RT-qPCR
mHP036	TTTCTTTAGTGGCCGTGGTG	Trp53bp1 reverse primer for RT-qPCR
mHP037	GTGTGGAGGAGGAGGAGTG	Bbc3 forward primer for RT-qPCR
mHP038	TCGATGCTGCTCTTCTTGTC	Bbc3 reverse primer for RT-qPCR
mHP039	GAGTGCACCGGACATAACTG	Pmaip1 forward primer for RT-qPCR
mHP040	CTCGTCCTTCAAGTCTGCTG	Pmaip1 reverse primer for RT-qPCR
mHP041	ATCTCAGTGCAATGGCTTCCA	Bcl2l11 (Bim) forward primer for RT-qPCR
mHP042	CTCCTGTGCAATCCGTATCT	Bcl2l11 (Bim) reverse primer for RT-qPCR
mHP043	AGACGAGCTGCAGACAGATG	Bid forward primer for RT-qPCR
mHP044	GGTCCATCTCATCGCCTATT	Bid reverse primer for RT-qPCR
mHP045	GGGGCCTTTTTGCTACAGGG	Bax forward primer for RT-qPCR
mHP046	AAAGATGGTCACTGTCTGCC	Bax reverse primer for RT-qPCR
mHP047	TTGTCGGCACAGAACAGAAG	Tsc1 forward primer for RT-qPCR
mHP048	TCAATGCCAGACCCAAAAGC	Tsc1 reverse primer for RT-qPCR
mHP049	TGACCTCAACTACATGGTCTACA	Gapdh forward primer for RT-qPCR
mHP050	CTTCCCATTCTCGGCCTTG	Gapdh reverse primer for RT-qPCR

Appendix B

Additional Results

B.1 Population-level

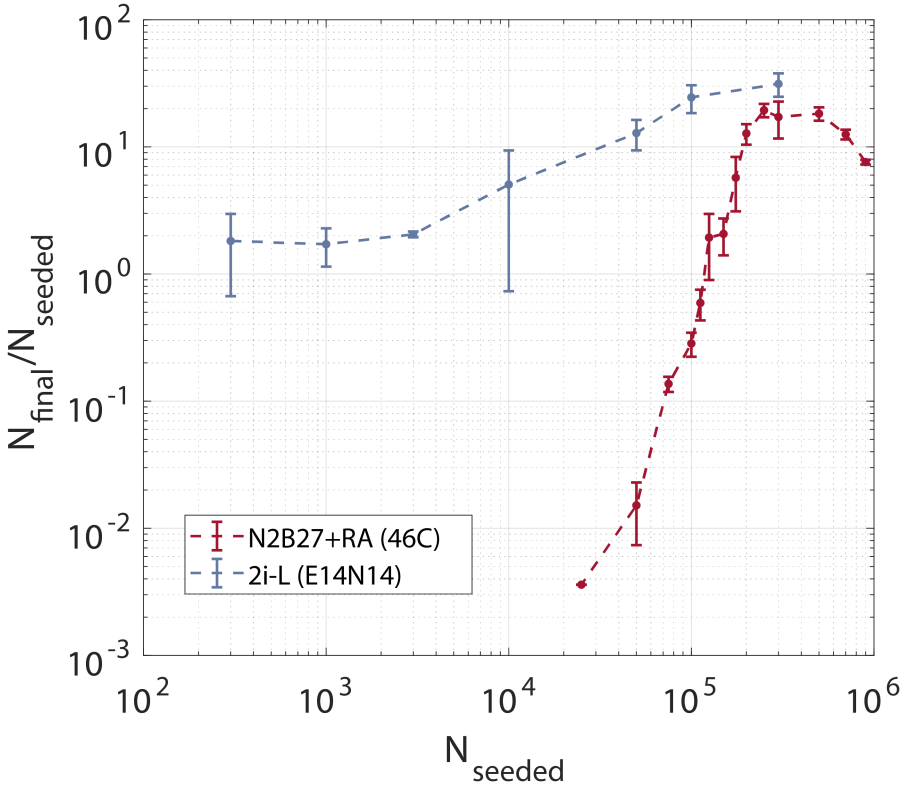

FIGURE B.1: Plot of growth ($\frac{N_{final}}{N_{seeded}}$) versus the seeded number of cells N_{seeded}. Cells were plated on a $\varnothing 10cm$ dish in different types of media, the media was refreshed on day two. Six days after plating N_{final} was measured using a hemocytometer. A condition in which cells are grown in N2B27+2i-LIF shows density independent behaviour. Condition with 46C in N2B27+RA shown for reference. Colours represent the different conditions and cell lines.Error bars represent the standard error of the mean of a minimum of three biological replicates.

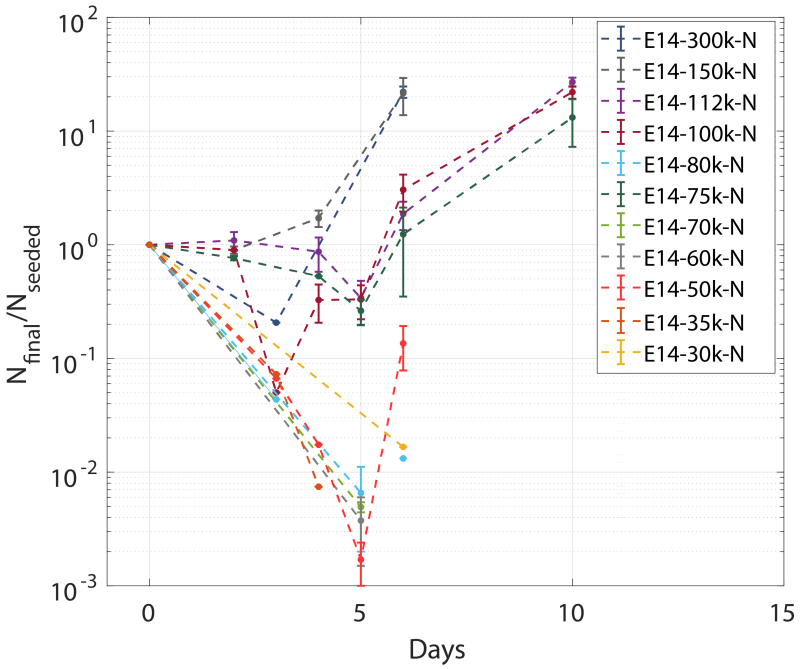

FIGURE B.2: Growth dynamics over a timespan of up to ten days for the E14 cell lines. Cells were grown on a $\varnothing 10cm$ dish in N2B27 medium which was refreshed with fresh N2B27 on day 2. N_{final} was measured using a hemocytometer. The legend represent the initial number of seeded cells with $k = 1000$. Error bars represent standard error of the mean.

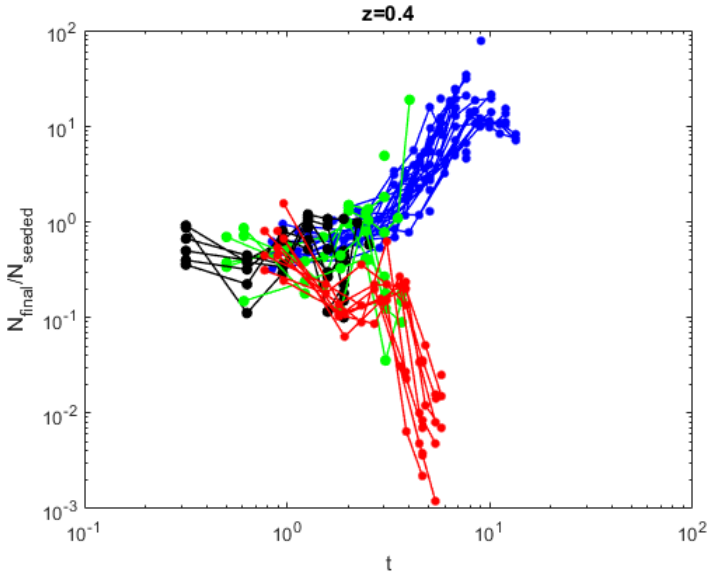

FIGURE B.3: Rescaled plot of 46C growth dynamics. Time was rescaled by $t = t \cdot |1 - \frac{N_t}{N_{Threshold}}|^z$ with z=0.4. Blue lines represent N_{seeded} larger than $N_{threshold}$, Red lines represent N_{seeded} smaller than $N_{threshold}$. Green lines represent N_{seeded} closer to $N_{threshold}$ and the black line represent the N_{seeded} which are closest to the $N_{threshold}$.

B.2 Colony-level

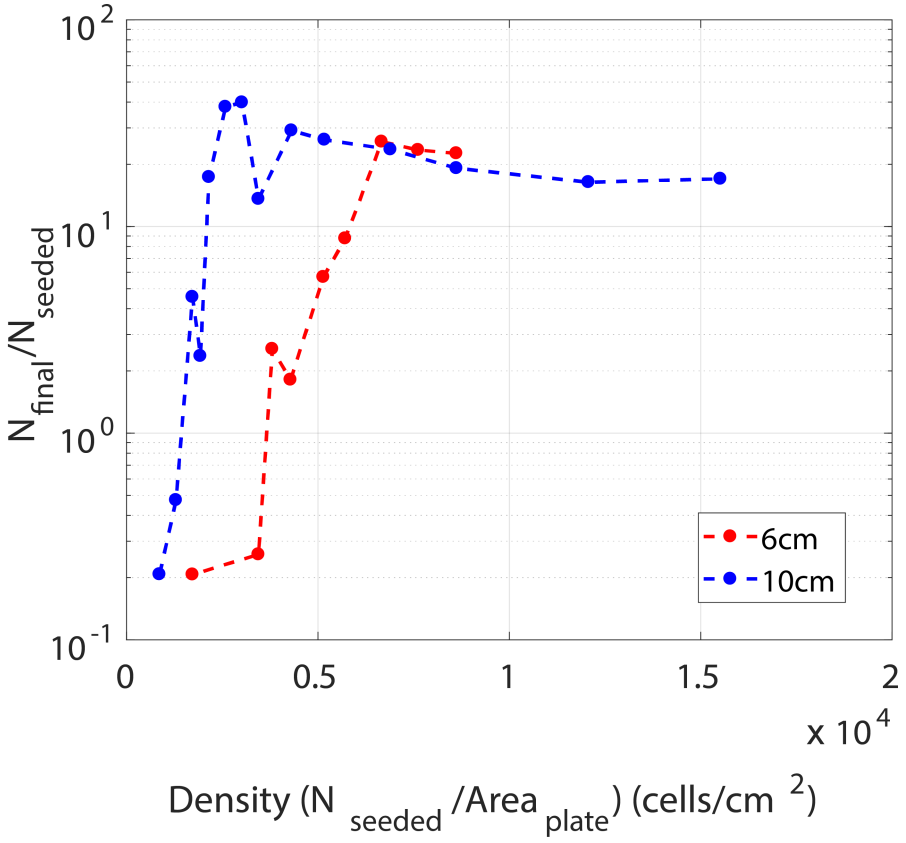

FIGURE B.4: Calibration curve ($\frac{N_{final}}{N_{seeded}}$) versus the seeded density $N_{seeded}/Area_{plate}$ for E14 cells grown on a $\varnothing 6cm$ (red) and $\varnothing 10cm$ (blue) plate. Cells were grown in N2B27 medium which was refreshed with fresh N2B27 on day 2. N_{final} was measured using a hemocytometer. Only 1 biological replicate is shown. This calibration curve shows that the conversion of the N_{seeded} of $\varnothing 10cm$ plates to the N_{seeded} on a $\varnothing 6cm$ plate is not as simple as multiplying the N_{seeded} with the ratio of the areas of the plates.

B.3 The Search for a Molecular Mechanism

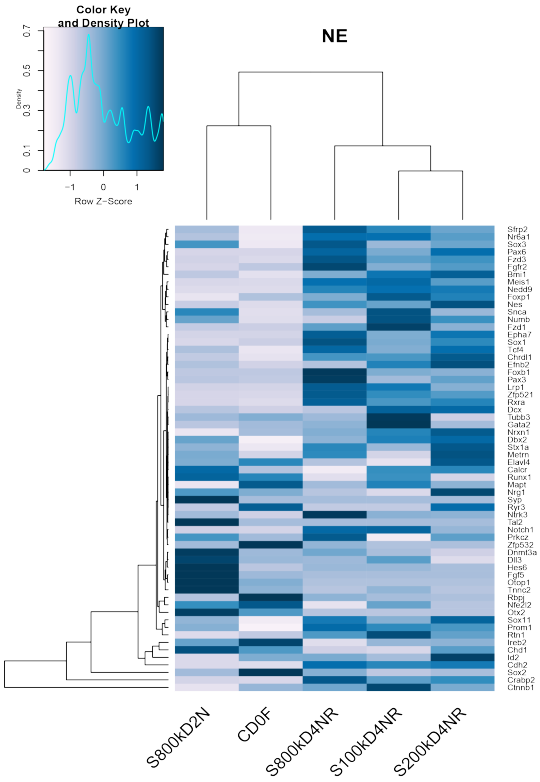

FIGURE B.5: Heatmap showing expression of neural ectoderm genes for the five different conditions. The conditions consist of a pluripotent control (CD0F), $N_{seeded} = 800k$ grown for two days in N2B27 (S800kD2N) and $N_{seeded} = 800k$ (S800kD4NR), $N_{seeded} = 200k$ (S200kD4NR), $N_{seeded} = 100k$ (S100kD4NR) grown for four days in N2B27, refreshing the media on day two with N2B27+RA. Light blue represents low expression and dark blue represents high expression.

B.4 A Model for Collective Survival

Parameter values for reaction-diffusion equation	
Parameter	**Value**
D_M	1000 ($\mu m^2/s$)
η	10 (mol/s)
γ	100 (1/s)
R	0.5 (μm)

Appendix C

Protocols for maintaining mESCs

C.1 Thawing and Plating mESCs

1. Label $\varnothing 10cm$ petri dish with name/date/cell line.
2. Evenly spread 10 ml 0.1% gelatin on the dish surface.
3. Incubate plate at $37°C$, for 30 minutes.
4. Add 10 ml pre-warmed pluripotency medium (S+L,2i+L depending on the cell line) in a tube.
5. Remove the gelatin from the dish.
6. Spread 5ml pre-warmed pluripotency medium on the dish.
7. Take 1 cryovial from the stock, and partially thaw until a pea-size frozen portion remains (30-60 s).
8. Transfer the cell/DMSO mixture (1 ml) into the tube with 5 ml of pre-warmed medium. An additional 1 ml of medium can be added to the empty cryovial, in order to dissolve and transfer the left-over cells.
9. Spin down the cells by centrifuging the tube at 200 x g to get rid of the DMSO.
10. Wash the cells twice by resuspending the cells in 1X PBS and spinning them down at 200x g.
11. After the last wash spin, resuspend cells in 5ml pluripotency medium.
12. Transfer the medium with cells to the plate.
13. To evenly spread the cells over the plate, gently shake the plate back and forth then left to right, allowing time for the , medium to settle between shakes.
14. Incubate plate with cells at $37°C$ and $5\%CO_2$.

C.2 Passaging mESCs

1. Label $\varnothing 10cm$ petri dish with name/date/cell line.
2. Evenly spread 10 ml 0.1% gelatin on the dish surface.
3. Incubate plate at $37°C$, for 30 minutes.
4. Take plate with cells that need to be passaged out of incubator.
5. Aspirate off medium and wash with 10ml 1X PBS.
6. Aspirate off PBS.
7. Spread 1ml accutase over the plate and incubate cells at $37°C$, for 5 minutes.
8. Take plate out, gently tap the plate to loosen the cells.
9. Pipet 1ml accutase with cells in a tube
10. Wash the plate off with 1ml 1X PBS to get the remaining cells that are stuck to the plate, pipette the 1 ml 1X PBS containing the cells into the tube. Repeat this step if necessary
11. Add 1X PBS to the tube with cells until you have a volume of 10ml.
12. Wash the cells twice by resuspending the cells in 1X PBS and spinning them down at 200x g.
13. After the last wash spin, resuspend cells in 1ml pluripotency medium (S+L,2i+L depending on the cell line).
14. Prepare a second tube with 10ml pluripotency medium and add 100 μl cells (1:10 dilution).
15. Take gelatin plate out of incubator
16. Aspirate off gelatin
17. Transfer the medium with cells to the plate.
18. To evenly spread the cells over the plate, gently shake the plate back and forth then left to right, allowing time for the , medium to settle between shakes.
19. Incubate plate with cells at $37°C$ and $5\%CO_2$.

Bibliography

[1] John T Emlen. Flocking behavior in birds. *The Auk*, 69(2):160–170, 1952.

[2] DV Radakov. Schooling in the echology of fish, israeli scientific translation series, 1973.

[3] Chris R Reid, Matthew J Lutz, Scott Powell, Albert B Kao, Iain D Couzin, and Simon Garnier. Army ants dynamically adjust living bridges in response to a cost–benefit trade-off. *Proceedings of the National Academy of Sciences*, 112(49):15113–15118, 2015.

[4] Maria Luisa Cotrina, Jane H-C Lin, Alexandra Alves-Rodrigues, Shujun Liu, Jiang Li, Hooman Azmi-Ghadimi, Jian Kang, Christian CG Naus, and Maiken Nedergaard. Connexins regulate calcium signaling by controlling atp release. *Proceedings of the National Academy of Sciences*, 95(26):15735–15740, 1998.

[5] Kenneth H Nealson, Terry Platt, and J Woodland Hastings. Cellular control of the synthesis and activity of the bacterial luminescent system. *Journal of bacteriology*, 104(1):313–322, 1970.

[6] Hyun Youk and Wendell A Lim. Secreting and sensing the same molecule allows cells to achieve versatile social behaviors. *Science*, 343(6171):1242782, 2014.

[7] Anne E Warner, Sarah C Guthrie, and Norton B Gilula. Antibodies to gap-junctional protein selectively disrupt junctional communication in the early amphibian embryo. *Nature*, 311(5982):127, 1984.

[8] Hans Spemann and Hilde Mangold. Über induktion von embryonalanlagen durch implantation artfremder organisatoren. *Archiv für mikroskopische Anatomie und Entwicklungsmechanik*, 100(3-4):599–638, 1924.

[9] Jaeseob Kim, Angela Sebring, Jeffrey J Esch, Mary Ellen Kraus, Kathy Vorwerk, Jeffrey Magee, and Sean B Carroll. Integration of positional signals and regulation of wing formation and identity by drosophila vestigial gene. *Nature*, 382(6587):133, 1996.

[10] Michael Cohen, Marios Georgiou, Nicola L Stevenson, Mark Miodownik, and Buzz Baum. Dynamic filopodia transmit intermittent delta-notch signaling to drive pattern refinement during lateral inhibition. *Developmental cell*, 19(1):78–89, 2010.

[11] Juan Carlos Fierro-González, Melanie D White, Juan Carlos Silva, and Nicolas Plachta. Cadherin-dependent filopodia control preimplantation embryo compaction. *Nature cell biology*, 15(12):1424, 2013.

[12] Andrzej K Tarkowski and Joanna Wróblewska. Development of blastomeres of mouse eggs isolated at the 4-and 8-cell stage. *Development*, 18(1):155–180, 1967.

[13] Nami Motosugi, Tobias Bauer, Zbigniew Polanski, Davor Solter, and Takashi Hiiragi. Polarity of the mouse embryo is established at blastocyst and is not prepatterned. *Genes & development*, 19(9):1081–1092, 2005.

[14] Lisa C Barcroft, Hanne Offenberg, Preben Thomsen, and Andrew J Watson. Aquaporin proteins in murine trophectoderm mediate transepithelial water movements during cavitation. *Developmental biology*, 256(2):342–354, 2003.

[15] PPL Tam and RSP Beddington. Establishment and organization of germ layers in the gastrulating mouse embryo. *Postimplantation development in the mouse*, 165:27–49, 1992.

[16] Claire Chazaud, Yojiro Yamanaka, Tony Pawson, and Janet Rossant. Early lineage segregation between epiblast and primitive endoderm in mouse blastocysts through the grb2-mapk pathway. *Developmental cell*, 10(5):615–624, 2006.

[17] Samantha A Morris, Roy TY Teo, Huiliang Li, Paul Robson, David M Glover, and Magdalena Zernicka-Goetz. Origin and formation of the first two distinct cell types of the inner cell mass in the mouse embryo. *Proceedings of the National Academy of Sciences*, page 200915063, 2010.

[18] David G Wilkinson, Sangita Bhatt, and Bernhard G Herrmann. Expression pattern of the mouse t gene and its role in mesoderm formation. *Nature*, 343(6259):657–659, 1990.

[19] Simon J Kinder, Tania E Tsang, Gabriel A Quinlan, Anna-Katerina Hadjantonakis, Andras Nagy, and PP Tam. The orderly allocation of mesodermal cells to the extraembryonic structures and the anteroposterior axis during gastrulation of the mouse embryo. *Development*, 126(21):4691–4701, 1999.

[20] Larysa H Pevny, Shantini Sockanathan, Marysia Placzek, and Robin Lovell-Badge. A role for sox1 in neural determination. *Development*, 125(10):1967–1978, 1998.

[21] Takeshi Fujiwara, Deborah B Dehart, Kathleen K Sulik, and Brigid LM Hogan. Distinct requirements for extra-embryonic and embryonic bone morphogenetic protein 4 in the formation of the node and primitive streak and coordination of left-right asymmetry in the mouse. *Development*, 129(20):4685–4696, 2002.

[22] Linda A Lowe, Satoru Yamada, and Michael R Kuehn. Genetic dissection of nodal function in patterning the mouse embryo. *Development*, 128(10):1831–1843, 2001.

[23] Pentao Liu, Maki Wakamiya, Martin J Shea, Urs Albrecht, Richard R Behringer, and Allan Bradley. Requirement for wnt3 in vertebrate axis formation. *Nature genetics*, 22(4):361, 1999.

[24] Chu-Xia Deng, Anthony Wynshaw-Boris, Michael M Shen, Cathie Daugherty, David M Ornitz, and Philip Leder. Murine fgfr-1 is required for early postimplantation growth and axial organization. *Genes & development*, 8(24):3045–3057, 1994.

[25] Martin J Evans and Matthew H Kaufman. Establishment in culture of pluripotential cells from mouse embryos. *nature*, 292(5819):154, 1981.

[26] Gail R Martin. Isolation of a pluripotent cell line from early mouse embryos cultured in medium conditioned by teratocarcinoma stem cells. *Proceedings of the National Academy of Sciences*, 78(12):7634–7638, 1981.

[27] Allan Bradley, Martin Evans, Matthew H Kaufman, and Elizabeth Robertson. Formation of germ-line chimaeras from embryo-derived teratocarcinoma cell lines. *Nature*, 309(5965):255, 1984.

[28] Michael R Kuehn, Allan Bradley, Elizabeth J Robertson, and Martin J Evans. A potential animal model for lesch–nyhan syndrome through introduction of hprt mutations into mice. *Nature*, 326(6110):295, 1987.

[29] James A Thomson, Joseph Itskovitz-Eldor, Sander S Shapiro, Michelle A Waknitz, Jennifer J Swiergiel, Vivienne S Marshall, and Jeffrey M Jones. Embryonic stem cell lines derived from human blastocysts. *science*, 282(5391):1145–1147, 1998.

[30] Geeta Shroff and Rakesh Gupta. Human embryonic stem cells in the treatment of patients with spinal cord injury. *Annals of neurosciences*, 22(4):208, 2015.

[31] Kazutoshi Takahashi and Shinya Yamanaka. Induction of pluripotent stem cells from mouse embryonic and adult fibroblast cultures by defined factors. *cell*, 126(4):663–676, 2006.

[32] Kazutoshi Takahashi, Koji Tanabe, Mari Ohnuki, Megumi Narita, Tomoko Ichisaka, Kiichiro Tomoda, and Shinya Yamanaka. Induction of pluripotent stem cells from adult human fibroblasts by defined factors. *cell*, 131(5):861–872, 2007.

[33] Jennifer Nichols, Branko Zevnik, Konstantinos Anastassiadis, Hitoshi Niwa, Daniela Klewe-Nebenius, Ian Chambers, Hans Schöler, and Austin Smith. Formation of pluripotent stem cells in the mammalian embryo depends on the pou transcription factor oct4. *Cell*, 95(3):379–391, 1998.

[34] Hitoshi Niwa, Jun-ichi Miyazaki, and Austin G Smith. Quantitative expression of oct-3/4 defines differentiation, dedifferentiation or self-renewal of es cells. *Nature genetics*, 24(4):372, 2000.

[35] Ariel A Avilion, Silvia K Nicolis, Larysa H Pevny, Lidia Perez, Nigel Vivian, and Robin Lovell-Badge. Multipotent cell lineages in early mouse development depend on sox2 function. *Genes & development*, 17(1):126–140, 2003.

[36] Shinji Masui, Yuhki Nakatake, Yayoi Toyooka, Daisuke Shimosato, Rika Yagi, Kazue Takahashi, Hitoshi Okochi, Akihiko Okuda, Ryo Matoba, Alexei A Sharov, et al. Pluripotency governed by sox2 via regulation of oct3/4 expression in mouse embryonic stem cells. *Nature cell biology*, 9(6):625, 2007.

[37] Kaoru Mitsui, Yoshimi Tokuzawa, Hiroaki Itoh, Kohichi Segawa, Mirei Murakami, Kazutoshi Takahashi, Masayoshi Maruyama, Mitsuyo Maeda, and Shinya Yamanaka. The homeoprotein nanog is required for maintenance of pluripotency in mouse epiblast and es cells. *cell*, 113(5):631–642, 2003.

[38] Ian Chambers, Douglas Colby, Morag Robertson, Jennifer Nichols, Sonia Lee, Susan Tweedie, and Austin Smith. Functional expression cloning of nanog, a pluripotency sustaining factor in embryonic stem cells. *Cell*, 113(5):643–655, 2003.

[39] Ian Chambers, Jose Silva, Douglas Colby, Jennifer Nichols, Bianca Nijmeijer, Morag Robertson, Jan Vrana, Ken Jones, Lars Grotewold, and Austin Smith. Nanog safeguards pluripotency and mediates germline development. *Nature*, 450(7173):1230, 2007.

[40] Joon-Lin Chew, Yuin-Han Loh, Wensheng Zhang, Xi Chen, Wai-Leong Tam, Leng-Siew Yeap, Pin Li, Yen-Sin Ang, Bing Lim, Paul Robson, et al. Reciprocal transcriptional regulation of pou5f1 and sox2 via the oct4/sox2 complex in embryonic stem cells. *Molecular and cellular biology*, 25(14):6031–6046, 2005.

[41] Yuin-Han Loh, Qiang Wu, Joon-Lin Chew, Vinsensius B Vega, Weiwei Zhang, Xi Chen, Guillaume Bourque, Joshy George, Bernard Leong, Jun Liu, et al. The oct4 and nanog transcription network regulates pluripotency in mouse embryonic stem cells. *Nature genetics*, 38(4):431, 2006.

[42] Sayaka Okumura-Nakanishi, Motoki Saito, Hitoshi Niwa, and Fuyuki Ishikawa. Oct-3/4 and sox2 regulate oct3/4 gene in es cells. *Journal of Biological chemistry*, 2004.

[43] Takao Kuroda, Masako Tada, Hiroshi Kubota, Hironobu Kimura, Shin-ya Hatano, Hirofumi Suemori, Norio Nakatsuji, and Takashi Tada. Octamer and sox elements are required for transcriptional cis regulation of nanog gene expression. *Molecular and cellular biology*, 25(6):2475–2485, 2005.

[44] R Lindsay Williams, Douglas J Hilton, Shirley Pease, Tracy A Willson, Colin L Stewart, David P Gearing, Erwin F Wagner, Donald Metcalf, Nicos A Nicola, and Nicholas M Gough. Myeloid leukaemia inhibitory factor maintains the developmental potential of embryonic stem cells. *Nature*, 336(6200):684, 1988.

[45] Austin G Smith, John K Heath, Deborah D Donaldson, Gordon G Wong, J Moreau, Mark Stahl, and David Rogers. Inhibition of pluripotential embryonic stem cell differentiation by purified polypeptides. *Nature*, 336(6200):688, 1988.

[46] Hitoshi Niwa, Tom Burdon, Ian Chambers, and Austin Smith. Self-renewal of pluripotent embryonic stem cells is mediated via activation of stat3. *Genes & development*, 12(13):2048–2060, 1998.

[47] Thi-Sau Migone, Scott Rodig, Nicholas A Cacalano, Maria Berg, Robert D Schreiber, and Warren J Leonard. Functional cooperation of the interleukin-2 receptor β chain and jak1 in phosphatidylinositol 3-kinase recruitment and phosphorylation. *Molecular and cellular biology*, 18(11):6416–6422, 1998.

[48] William P Schiemann, Joseph L Bartoe, and Neil M Nathanson. Box 3-independent signaling mechanisms are involved in leukemia inhibitory factor receptor α-and gp130-mediated stimulation of mitogen-activated protein kinase evidence for participation of multiple signaling pathways which converge at ras. *Journal of Biological Chemistry*, 272(26):16631–16636, 1997.

[49] Peter Cartwright, Cameron McLean, Allan Sheppard, Duane Rivett, Karen Jones, and Stephen Dalton. Lif/stat3 controls es cell self-renewal and pluripotency by a myc-dependent mechanism. *Development*, 132(5):885–896, 2005.

[50] Qi-Long Ying, Jason Wray, Jennifer Nichols, Laura Batlle-Morera, Bradley Doble, James Woodgett, Philip Cohen, and Austin Smith. The ground state of embryonic stem cell self-renewal. *Nature*, 453(7194):519, 2008.

[51] Qi-Long Ying, Jennifer Nichols, Ian Chambers, and Austin Smith. Bmp induction of id proteins suppresses differentiation and sustains embryonic stem cell self-renewal in collaboration with stat3. *Cell*, 115(3):281–292, 2003.

[52] Tilo Kunath, Marc K Saba-El-Leil, Marwa Almousailleakh, Jason Wray, Sylvain Meloche, and Austin Smith. Fgf stimulation of the erk1/2 signalling cascade triggers transition of pluripotent embryonic stem cells from self-renewal to lineage commitment. *Development*, 134(16):2895–2902, 2007.

[53] Marios P Stavridis, J Simon Lunn, Barry J Collins, and Kate G Storey. A discrete period of fgf-induced erk1/2 signalling is required for vertebrate neural specification. *Development*, 134(16):2889–2894, 2007.

[54] Atsushi Kubo, Katsunori Shinozaki, John M Shannon, Valerie Kouskoff, Marion Kennedy, Savio Woo, Hans Joerg Fehling, and Gordon Keller. Development of definitive endoderm from embryonic stem cells in culture. *Development*, 131(7):1651–1662, 2004.

[55] Paul Gadue, Tara L Huber, Patrick J Paddison, and Gordon M Keller. Wnt and tgf-β signaling are required for the induction of an in vitro model of primitive streak formation using embryonic stem cells. *Proceedings of the National Academy of Sciences*, 103(45):16806–16811, 2006.

[56] R Coleman Lindsley, Jennifer G Gill, Michael Kyba, Theresa L Murphy, and Kenneth M Murphy. Canonical wnt signaling is required for development of embryonic stem cell-derived mesoderm. *Development*, 133(19):3787–3796, 2006.

[57] Heather B Wood and Vasso Episkopou. Comparative expression of the mouse sox1, sox2 and sox3 genes from pre-gastrulation to early somite stages. *Mechanisms of development*, 86(1):197–201, 1999.

[58] Jerôme Aubert, Hannah Dunstan, Ian Chambers, and Austin Smith. Functional gene screening in embryonic stem cells implicates wnt antagonism in neural differentiation. *Nature biotechnology*, 20(12):1240, 2002.

[59] Qi-Long Ying, Marios Stavridis, Dean Griffiths, Meng Li, and Austin Smith. Conversion of embryonic stem cells into neuroectodermal precursors in adherent monoculture. *Nature biotechnology*, 21(2):183, 2003.

[60] Marios P Stavridis, Barry J Collins, and Kate G Storey. Retinoic acid orchestrates fibroblast growth factor signalling to drive embryonic stem cell differentiation. *Development*, 137(6):881–890, 2010.

[61] Matt Thomson, Siyuan John Liu, Ling-Nan Zou, Zack Smith, Alexander Meissner, and Sharad Ramanathan. Pluripotency factors in embryonic stem cells regulate differentiation into germ layers. *Cell*, 145(6):875–889, 2011.

[62] Sergei Y Sokol. Maintaining embryonic stem cell pluripotency with wnt signaling. *Development*, pages dev–066209, 2011.

[63] Hanjun Kim, Sewoon Kim, Yonghee Song, Wantae Kim, Qi-Long Ying, and Eekhoon Jho. Dual function of wnt signaling during neuronal differentiation of mouse embryonic stem cells. *Stem cells international*, 2015, 2015.

[64] Martin Hooper, Kate Hardy, Alan Handyside, Susan Hunter, and Marilyn Monk. Hprt-deficient (lesch–nyhan) mouse embryos derived from germline colonization by cultured cells. *Nature*, 326(6110):292, 1987.

[65] Hans Jörg Fehling, Georges Lacaud, Atsushi Kubo, Marion Kennedy, Scott Robertson, Gordon Keller, and Valerie Kouskoff. Tracking mesoderm induction and its specification to the hemangioblast during embryonic stem cell differentiation. *Development*, 130(17):4217–4227, 2003.

[66] Kathryn C Davidson, Allison M Adams, Jamie M Goodson, Circe E McDonald, Jennifer C Potter, Jason D Berndt, Travis L Biechele, Russell J Taylor, and Randall T Moon. Wnt/β-catenin signaling promotes differentiation, not self-renewal, of human embryonic stem cells and is repressed by oct4. *Proceedings of the National Academy of Sciences*, page 201118777, 2012.

[67] Kenneth J Livak and Thomas D Schmittgen. Analysis of relative gene expression data using real-time quantitative pcr and the 2- $\delta\delta$ct method. *methods*, 25(4):402–408, 2001.

[68] Ben Langmead, Cole Trapnell, Mihai Pop, and Steven L Salzberg. Ultrafast and memory-efficient alignment of short dna sequences to the human genome. *Genome biology*, 10(3):R25, 2009.

[69] Cole Trapnell, Lior Pachter, and Steven L Salzberg. Tophat: discovering splice junctions with rna-seq. *Bioinformatics*, 25(9):1105–1111, 2009.

[70] Cole Trapnell, Brian A Williams, Geo Pertea, Ali Mortazavi, Gordon Kwan, Marijke J Van Baren, Steven L Salzberg, Barbara J Wold, and Lior Pachter. Transcript assembly and quantification by rna-seq reveals unannotated transcripts and isoform switching during cell differentiation. *Nature biotechnology*, 28(5):511, 2010.

[71] Kenneth T Frank, Brian Petrie, Jae S Choi, and William C Leggett. Trophic cascades in a formerly cod-dominated ecosystem. *Science*, 308(5728):1621–1623, 2005.

[72] Warder Clyde Allee, Orlando Park, Alfred Edwards Emerson, Thomas Park, Karl Patterson Schmidt, et al. Principles of animal ecology. Technical report, WB Saunders Philadelphia, 1949.

[73] C Wissel. A universal law of the characteristic return time near thresholds. *Oecologia*, 65(1):101–107, 1984.

[74] Egbert H van Nes and Marten Scheffer. Implications of spatial heterogeneity for catastrophic regime shifts in ecosystems. *Ecology*, 86(7):1797–1807, 2005.

[75] D Duval, M Malaise, B Reinhardt, C Kedinger, and H Boeuf. A p38 inhibitor allows to dissociate differentiation and apoptotic processes triggered upon lif withdrawal in mouse embryonic stem cells. *Cell death and differentiation*, 11(3):331, 2004.

[76] Massimo De Felici, A Di Carlo, M Pesce, S Iona, MG Farrace, and M Piacentini. Bcl-2 and bax regulation of apoptosis in germ cells during prenatal oogenesis in the mouse embryo. *Cell death and differentiation*, 6(9):908, 1999.

[77] Eduardo P Olimpio, Yiteng Dang, and Hyun Youk. Statistical dynamics of spatial-order formation by communicating cells. *iScience*, 2:27–40, 2018.

[78] Colin L Stewart, Petr Kaspar, Lisa J Brunet, Harshida Bhatt, Inder Gadi, Frank Köntgen, and Susan J Abbondanzo. Blastocyst implantation depends on maternal expression of leukaemia inhibitory factor. *Nature*, 359(6390):76, 1992.

[79] Jennifer Nichols, Ian Chambers, Tetsuya Taga, and Austin Smith. Physiological rationale for responsiveness of mouse embryonic stem cells to gp130 cytokines. *Development*, 128(12):2333–2339, 2001.

[80] Nikhil Mittal and Joel Voldman. Nonmitogenic survival-enhancing autocrine factors including cyclophilin a contribute to density-dependent mouse embryonic stem cell growth. *Stem cell research*, 6(2):168–176, 2011.

[81] Ying Guo, Barbara Graham-Evans, and Hal E Broxmeyer. Murine embryonic stem cells secrete cytokines/growth modulators that enhance cell survival/anti-apoptosis and stimulate colony formation of murine hematopoietic progenitor cells. *Stem Cells*, 24(4):850–856, 2006.

[82] Kevin Thurley, Daniel Gerecht, Elfriede Friedmann, and Thomas Höfer. Three-dimensional gradients of cytokine signaling between t cells. *PLoS computational biology*, 11(4):e1004206, 2015.